INVESTIGATION OF CENTRIFUGAL FORCE AND REYNOLDS NUMBER EFFECTS ON COMBUSTION PROCESSES

George D. Lewis, et al

Pratt and Whitney Aircraft

Prepared for:

Air Force Office of Scientific Research

June 1975

UNCLASSIFIED

SECURITY CLASSIFICATION OF THIS PAGE *(When Data Entered)*

REPORT DOCUMENTATION PAGE		READ INSTRUCTIONS BEFORE COMPLETING FORM
1 REPORT NUMBER AFOSR - TR - 75 - 1167	2 GOVT ACCESSION NO.	3 RECIPIENT'S CATALOG NUMBER
4. TITLE *(and Subtitle)* INVESTIGATION OF CENTRIFUGAL FORCE AND REYNOLDS NUMBER EFFECTS ON COMBUSTION PROCESSES		5 TYPE OF REPORT & PERIOD COVERED FINAL June 1973 - June 1975 6 PERFORMING ORG. REPORT NUMBER P&WA FR-6996
7. AUTHOR(s) GEORGE D. LEWIS CLIFFORD E. SMITH		8 CONTRACT OR GRANT NUMBER(s) F44620-73-C-0061
9. PERFORMING ORGANIZATION NAME AND ADDRESS PRATT & WHITNEY AIRCRAFT/UNITED TECHNOLOGIES CORPORATION, FRDC BOX 2691, WEST PALM BEACH, FLORIDA 33402		10 PROGRAM ELEMENT, PROJECT, TASK AREA & WORK UNIT NUMBERS 681308 9711-02 61102F
11 CONTROLLING OFFICE NAME AND ADDRESS AIR FORCE OFFICE OF SCIENTIFIC RESEARCH/NA 1400 WILSON BOULEVARD ARLINGTON, VIRGINIA 22209		12 REPORT DATE June 1975 13 NUMBER OF PAGES 85
14 MONITORING AGENCY NAME & ADDRESS *(If different from Controlling Office)*		15 SECURITY CLASS. *(of this report)* UNCLASSIFIED 15a. DECLASSIFICATION/DOWNGRADING SCHEDULE

16 DISTRIBUTION STATEMENT *(of this Report)*

Approved for public release; distribution unlimited.

17. DISTRIBUTION STATEMENT *(of the abstract entered in Block 20, if different from Report)*

18 SUPPLEMENTARY NOTES

19 KEY WORDS *(Continue on reverse side if necessary and identify by block number)*

SWIRL
BUOYANCE
CENTRIFUGAL FORCE
COMBUSTION
EXTINCTION
COMBUSTION LIMITS

20 ABSTRACT *(Continue on reverse side if necessary and identify by block number)*

Tests in a combustion centrifuge have demonstrated that increased byoyance produced by centrifugal force can be used to increase flamespeeds significantly over turbulent flamespeed, which controls combustion rates in conventional burners. A model has been developed that predicts the flamespreading rate at various burner conditions. In addition, a second model, based on classical heat transfer correlations, has been developed to predict with reasonable accuracy the extinction limits of flames at very high centrifugal force values. The effects of Reynolds number on turbulent flamespeeds

DD FORM 1 JAN 73 1473 EDITION OF 1 NOV 65 IS OBSOLETE

UNCLASSIFIED

SECURITY CLASSIFICATION OF THIS PAGE *(When Data Entered)*

and on limiting bubble size in gravitational fields have also been measured. Testing of a subscale swirl augmentor has confirmed the validity of the experimental model and it has been used to design a full-scale swirl augmentor for advanced versions of an Air Force turbofan engine. The swirl augmentor is predicted to reduce the fuel consumption and increase the stability of the engine.

ABSTRACT

Tests in a combustion centrifuge have demonstrated that increased buoyancy produced by centrifugal force can be used to increase flamespeeds significantly over turbulent flamespeed, which controls combustion rates in conventional burners. A model has been developed that predicts the flamespreading rate at various burner conditions. In addition, a second model, based on classical heat transfer correlations, has been developed to predict with reasonable accuracy the extinction limits of flames at very high centrifugal force values. The effects of Reynolds number on turbulent flamespeeds and on limiting bubble sizes in gravitational fields have also been measured. Testing of a subscale swirl augmentor has confirmed the validity of the experimental model and it has been used to design a full-scale swirl augmentor for advanced versions of an Air Force turbofan engine. The swirl augmentor is predicted to reduce the fuel consumption and increase the stability of the engine.

CONTENTS

ILLUSTRATIONS

ILLUSTRATIONS (Continued)

TABLES

SECTION I
INTRODUCTION

There are two commonly accepted means of spreading flame through a combustible mixture in practical combustion systems. The first of these, laminar flame propagation, depends on heat conduction and the diffusion of chemically active species into the adjacent fuel-air mixture to propagate the fire. One foot per second is a typical laminar flamespeed for stoichiometric hydrocarbon-air mixtures. The second, turbulent flame propagation, adds the turbulent transport of small elements of flame a short distance into the unburned mixture to act as new ignition sources. Turbulent flamespeeds in hydrocarbon-air mixtures typically range from 2 to about 20 feet per second. In the past, when attempts have been made to increase the turbulent flamespeed to higher values, the pressure drop required to produce the turbulence has been prohibitive for practical applications, or flame stabilization problems prevented operation at higher velocities. Recently, tests in a combustion centrifuge have demonstrated that centrifugal force can be used to increase flame propagation rates by an additional factor of 4 or more. This report describes the analytical and experimental program conducted under Contract F44620-73-C-0061 with the Air Force Office of Scientific Research to provide a sound basis for applying this phenomenon to Air Force combustion problems.

SECTION II
RESEARCH PROGRAM

A 2-year combined analytical and experimental effort was aimed at a thorough understanding of the effects of centrifugal force on combustion and the development of a mathematical model that can be used as a design tool for Air Force combustion systems. The first year's work consisted of obtaining experimental data with the combustion centrifuge and comparing the results with those from other sources. A preliminary mathematical model was also developed. During the second year further experimental data on the behavior of buoyant fluids in a dense medium were obtained and refinement of the preliminary model was completed.

A. EXPERIMENTAL AND ANALYTICAL RESULTS

The experimental and analytical work consisted of four phases: (1) the spreading of flame through a combustible mixture by the buoyant movement of flame bubbles, (2) the extinction of flames in high centrifugal force fields, (3) the effects of Reynolds No. on turbulent flamespeed, and (4) application of the results. The four phases will be discussed separately.

1. Flamespreading

When a hydrocarbon fuel-air mixture burns, the heat released by the chemical reaction raises the temperature of the burned products and causes them to expand. The expansion results in a lower density of the burned products than for the unburned mixture. Gravitational and centrifugal forces tend to organize fluids of different densities, with the heaviest on the bottom and the lightest on top. This buoyant force causes the flame to rise from a burning candle in the earth's gravitational field. In more intense combustion systems, such as in a turbine engine burner, the buoyant forces produced by the earth's gravitational field are insignificant compared to the forces produced by the flowing air stream and do not measurably affect the combustion process. If the earth's gravitational field is supplemented by a centrifugal force field several thousand times stronger, the buoyant forces again become predominant and completely control the flame spreading process. The resulting buoyant force can be expressed as:

$$F_B = (\rho_a)\ (a)\left(1 - \frac{\rho_B}{\rho_a}\right) \qquad \text{Eq (1)}$$

where:

F_B is buoyant force per unit volume

a is gravitational or centrifugal acceleration

ρ_a is density of cold air

ρ_B is density of hot products of combustion.

This force is relatively weak in the earth's gravitational field. For example, it amounts to approximately 0.063 pound for a 1-foot cube of hot gas at ambient pressure having a temperature of 3500°F surrounded by air at 80°F. In a 3000-g centrifugal field, however, it becomes a force of 190 pounds on a cubic foot of gas. This large force completely dominates the movement of the flame within the combustor.

A series of basic experiments was conducted using a combustion centrifuge. The centrifuge was constructed from a 2.65-inch internal diameter (nominal 3-inch, heavy wall) stainless steel pipe, 6 feet long and closed at both ends with weld caps. An automotive-type spark plug is mounted at one end behind a turbulence generator, and a 2000-psi burst disk is located at the other end. The turbulence generator, consisting of a flat disk with holes in it, has 40% blockage and is placed 2-1/2 inches from the spark plug to ensure the generation of a fully turbulent flame before the fire reaches the instrumented section. Ionization probes are installed at the locations shown in figure 1, and a pressure transducer and a thermocouple are mounted near the center of the pipe. Flame propagation rate measurements are made between stations 1 and 11 to (1) provide a long test section to reduce the scatter from small, local flame speed variations, and (2) obtain data before much of the mass is burned and the pressure rise due to combustion becomes significant. Slip rings permit the continuous recording of 12 channels of information. An insulated brass disk and roller transmit the ignition energy from a variable energy ignition source to the spark plug. The entire unit is mounted on tapered roller bearings and can be rotated by a 400-horsepower, variable-speed electric motor. The assembly is shown in figure 2.

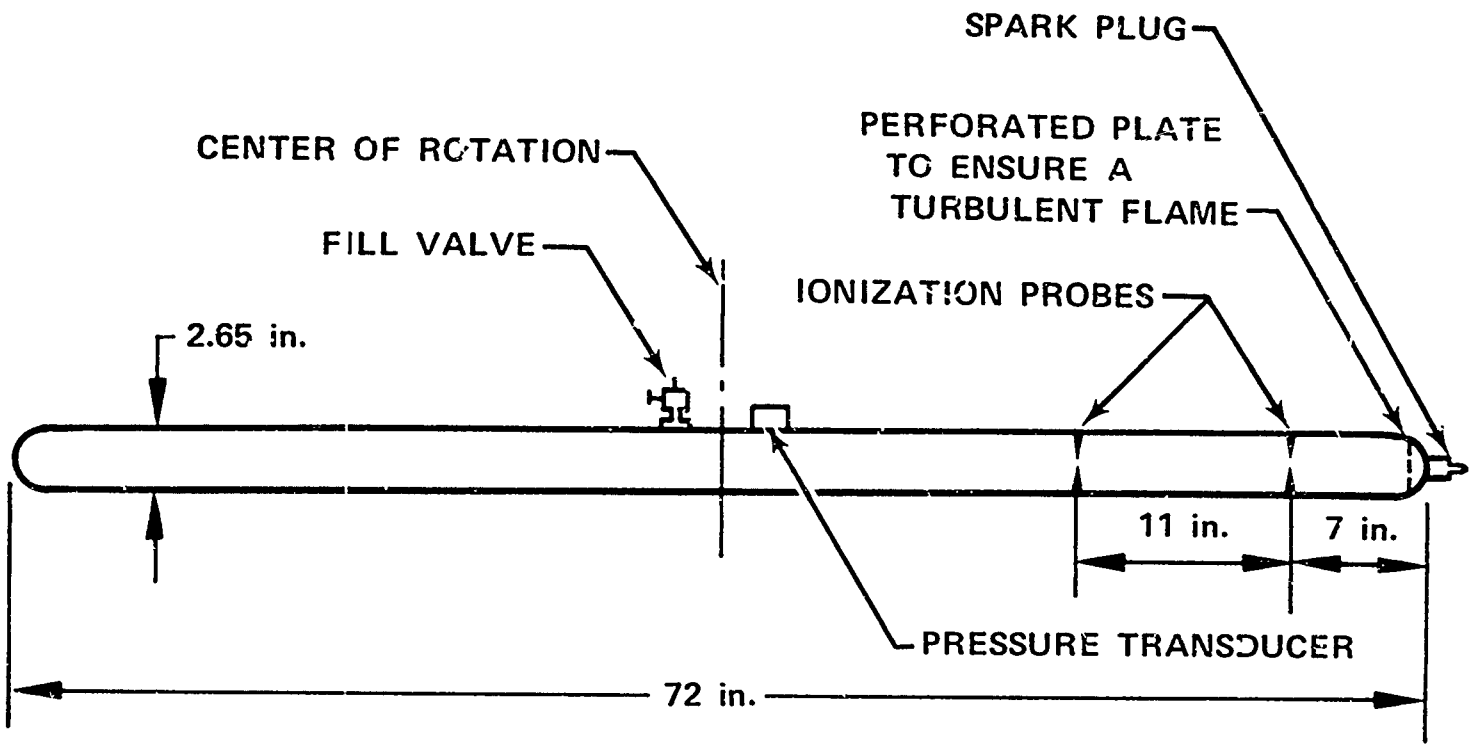

Figure 1. Combustion Centrifuge

FD 74051

Figure 2. Combustion Centrifuge Mounted on Test Stand FE 335060

The ionization probes are steel spikes mounted from opposite sides of the pipe, with one spike of a pair welded to the pipe and the other inserted through an insulating collar. The spikes are conical in shape to resist bending under the high centrifugal loads, and the points are separated by a 0.050-inch gap at the center of the pipe. A 90-volt electric potential is applied to each pair of spikes, and the flow of current that results when ionized flame completes the circuit is recorded on an oscillograph at a paper speed of 160 inches per second. Rotational speed is recorded on the oscillograph and also indicated on a digital display in the control room. The signal is generated by redundant reluctance pickups mounted adjacent to 60-tooth gears.

The fuel-air mixture is prepared in a separate tank and admitted to the centrifuge, one charge at a time. The mix tank and centrifuge are first evacuated to below 50-micron pressure and valved off to check for leaks. The mix tank is then isolated from the centrifuge and fuel is admitted to a predetermined pressure. Dry compressed air is added until the desired fuel-air ratio is reached, and an internally mounted paddle is oscillated to stir the mixture. One full tank can supply fuel-air mixture to the centrifuge for from 3 to 45 tests, depending on the pressure level being investigated. The centrifuge is enclosed in an insulated housing supplied with liquid nitrogen so that the temperatures of both the centrifuge and the surrounding gas can be varied from +200°F to -100°F.

To conduct a test, the centrifuge is evacuated to a 50-micron pressure to remove the products of combustion from prior testing, and a fuel-air charge is admitted to the desired pressure level. The mix tank is then valved off, and the transfer line disconnected and capped. The pipe is then rotated to the desired speed and either chilled by adding liquid nitrogen to the enclosure or heated by running it in the enclosure until mechanical energy of rotation has heated both the centrifuge and surrounding air to the desired temperature. Thermocouples in the enclosure and inside the centrifuge monitor the temperatures. After the desired temperature is reached, the spark is fired and the data are recorded on the oscillograph. The results for propane-air mixtures are presented in figure 3. The observed flame propagation rate is plotted as a function of the centrifugal acceleration at the igniter. The centrifugal acceleration midway between the ionization probes is about two-thirds of this value.

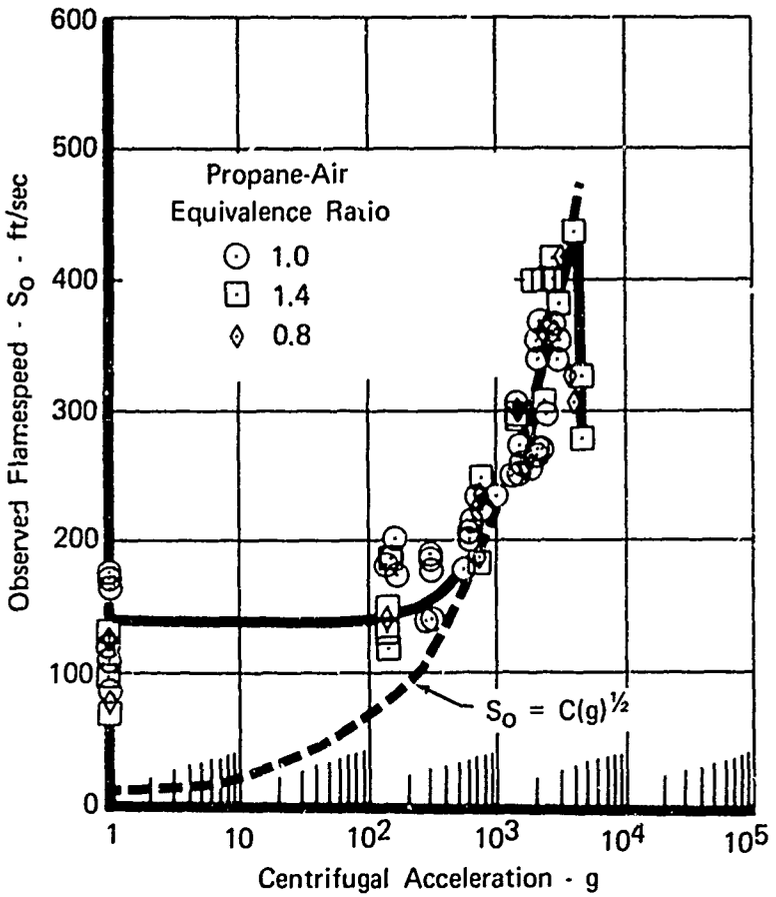

Figure 3. Observed Flamespeed as a Function of Centrifugal Acceleration for Propane Air Mixtures FD 74050

As figure 3 shows, the flame propagation rate is relatively unaffected by centrifugal acceleration up to about 200 g. Above this value, up to about 500 g, is a transition region. At values above 500 g, the observed flame propagation rate increases about in proportion to the square root of the centrifugal force. A dashed "square root curve" is added to figure 3 for comparison. Near 3500 g, a point is reached where the observed flamespeed abruptly reverses the trend. From here, it decreases with increasing centrifugal acceleration until a limit is reached beyond which combustion will not occur. Fuel-air mixture ratios other than the one plotted here exhibited the same behavior, although the maximum flamespeed and flame extinction points occurred at significantly different centrifugal acceleration values.

Tests with hydrogen-air mixtures yielded somewhat different results. A stoichiometric hydrogen-air mixture, at 1-atm precombustion pressure, showed a constant flame propagation rate over the range of centrifugal acceleration

values tested. When the mixture equivalence ratio was dropped to 0.6, however, the measured flame spreading rates corresponded very closely to those for propane-air mixtures at the same g values. The experimental data are presented in figure 4, along with data obtained from stoichiometric hydrogen-air mixtures at 0.33-atm precombustion pressure. Included for comparison is the mean curve through the propane-air data of figure 3. These contrasting sets of data imply that two different mechanisms control the flame spreading, and a hypothesis is proposed to explain them.

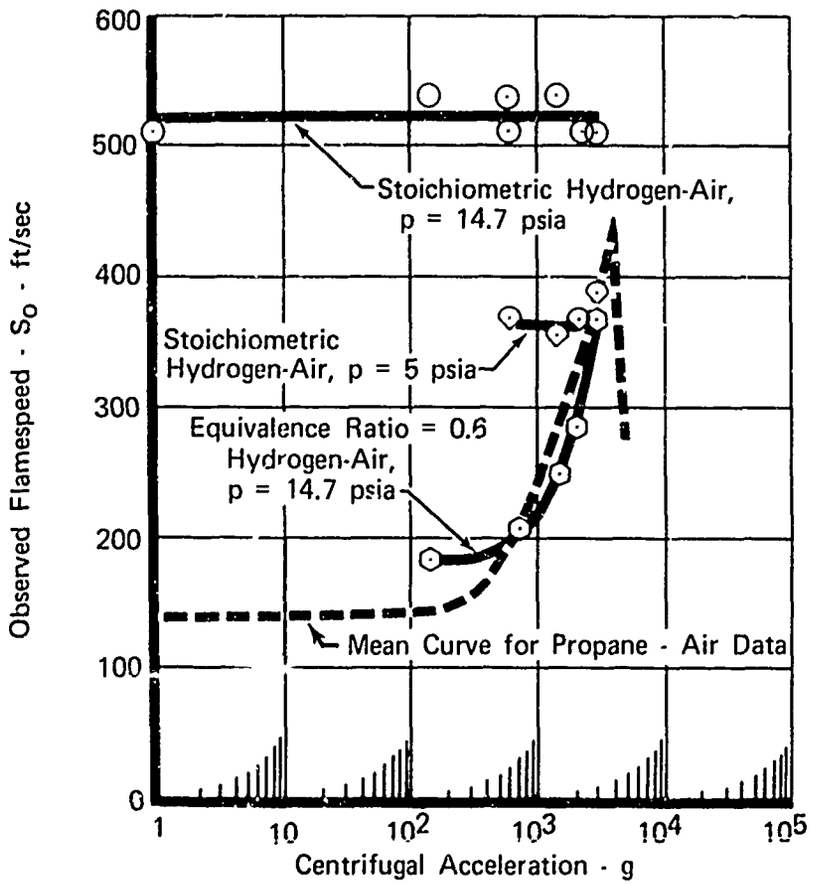

Figure 4. Observed Flamespeed as a Function of Centrifugal Acceleration for Hydrogen-Air Mixtures FD 74049

Figure 5 shows the situations schematically. A flame bubble immersed in a denser fuel-air mixture (represented by the cross-hatched circles) is displaced upward by the buoyant force resulting from a high centrifugal-force field and the density difference. In an increment of time, Δt, it moves a distance equal to the product of the time increment multiplied by the velocity, S_B, which will be called the "bubble velocity." During the same time, turbulent flame propagation has

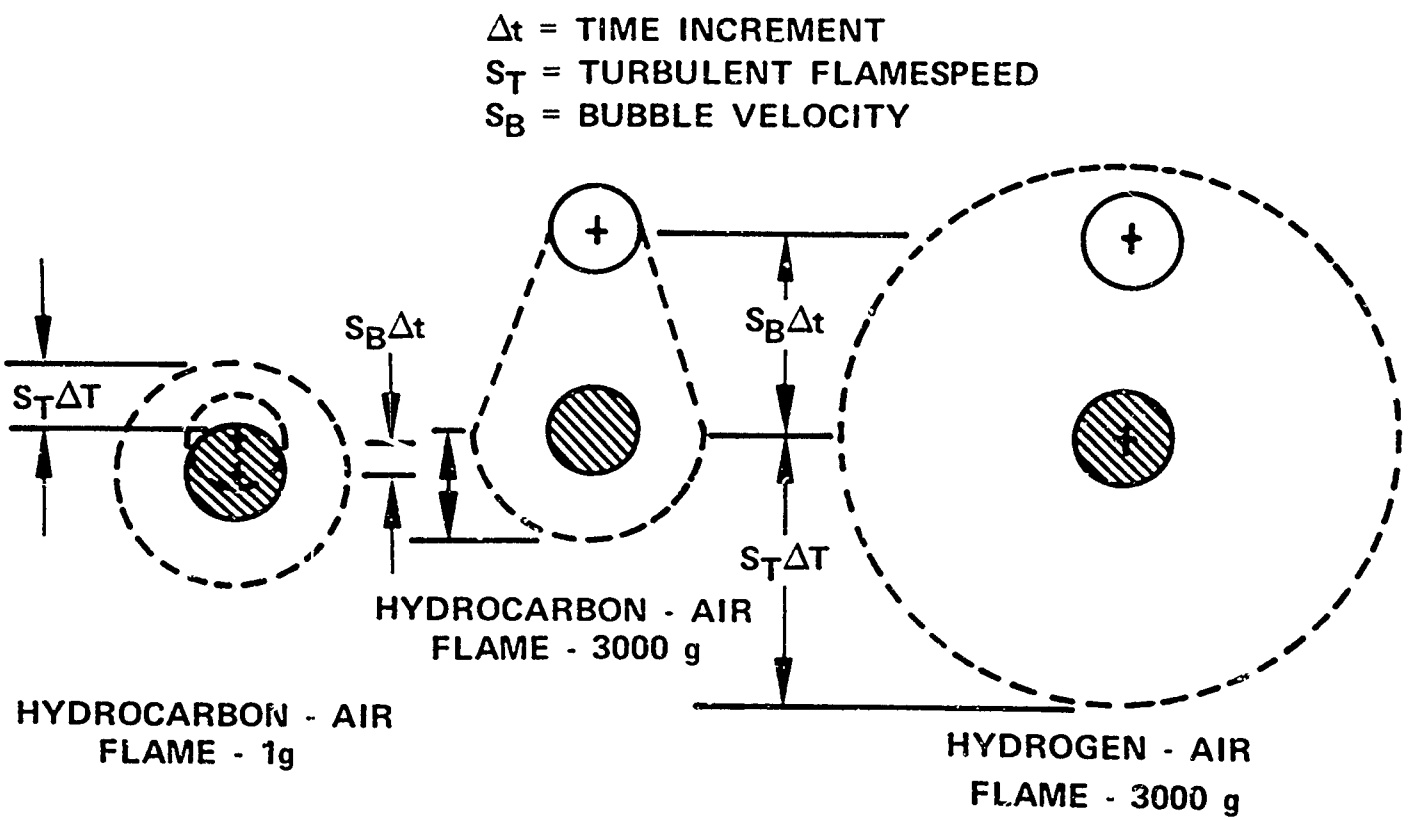

Figure 5. Schematic Comparison of Turbulent Flamespreading and Bubble Flamespreading FD 59829B

caused the flamefront to advance in all directions by an amount equal to the product of the turbulent flamespeed, S_T, multiplied by the same time increment. (Hot-gas expansion behind the flamefront is neglected for simplicity.) The example on the extreme left in figure 5 respresents the case where bubble velocity is negligible, as with stoichiometric propane-air combustion in the earth's gravitational field. The data near the left axis of figure 3 represent this condition. If a strong centrifugal force field is added, however, the bubble races ahead of the advancing turbulent flamefront, as shown in the middle sketch of figure 5. To an observer measuring flame propagation, the rate would depend only on centrifugal acceleration intensity. This is the situation represented by the data above about 500 g in figure 3. The sketch on the extreme right in figure 5 represents a case where a centrifugal force field is applied, but the turbulent flamespeed still exceeds the bubble velocity. The stoichiometric hydrogen-air data of figure 4 represent this case. Thus, it is apparent that the higher of the two velocities, either turbulent flamespeed or bubble velocity, determines the rate of flame propagation through a combustible mixture, and the other has no effect.

It should be noted that the observed flamespeed shown in figure 4 is not the true flamespeed through the cold mixture, but is the sum of the true flamespeed, S_B, plus the velocity of the unburned mixture through the pipe caused by the expansion of the burned gases. Based on the assumptions of no heat loss and 100% combustion efficiency, the expansion of the burned gas can be calculated and subtracted from the observed velocity to obtain the true velocity of the hot flame bubble through the cold fuel-air mixture. Figure 6 presents the bubble velocity calculated from the observed flame propagation rates.

As noted on the curve, above about 500 g the bubble velocity, S_B, can be represented by the equation

$$S_B = (1.25)\,(g_{\text{at igniter}})^{1/2} \qquad \text{Eq (2)}$$

for the conditions tested.

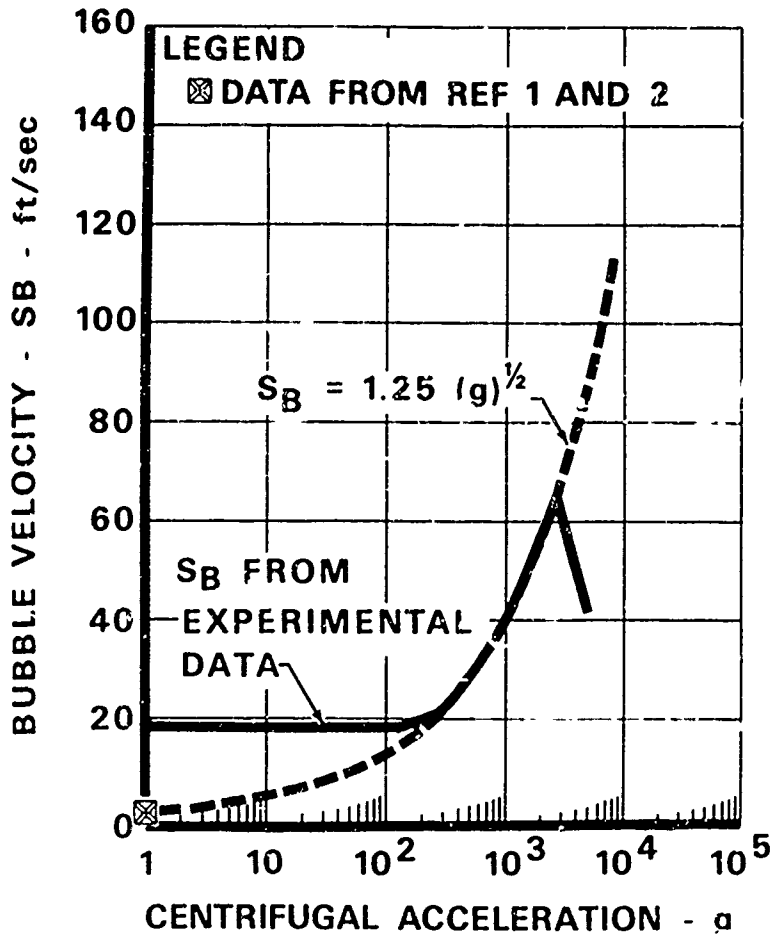

Figure 6. Flame Bubble Velocity as a Function of Centrifugal Acceleration FD 74048

Below about 200 g turbulent flamespeed controls flame propagation, and the rate is independent of centrifugal acceleration. It is interesting to note that, if Equation 2 is extended down to 1 g conditions, the bubble velocity is 1.25 feet per second. This velocity agrees very closely with published measurements of air bubbles in water (Reference 1) and flame bubbles in cold fuel-air mixtures (Reference 2) near the lean fuel-air ratio limit, where the normal flamespeed is low enough for buoyant forces to become dominant even at 1 g conditions. Additional calculations of true flamespeed based on the measured rate of pressure rise near the beginning of combustion gave similar, but generally higher, flamespeed values.

Additional tests were run to determine the pressure effect on flamespeed. These tests, presented in figure 7, showed that the flamespreading process is independent of pressure between 75 psia and 5 psia. Below 5 psia, the experimental data deviate significantly from those at higher pressure, probably as a result of the increasing ratio of heat lost to heat generated as the pressure is reduced.

All of the flamespreading experimental data obtained under the current contract are tabulated in Appendix A.

a. Development of Analytical Model

An analytical model based on basic bubble mechanics was formulated to predict the observed flamespreading rates. From Newton's law of motion on the flame bubble, the buoyant force and drag force must equate to the mass times the acceleration of the bubble. In equation form this can be written as:

$$\left(\rho_B\right)\left(V_B\right)\left(\frac{d^2R}{dt^2}\right) = \left(-R\omega^2\right)\left(\rho_a\right)\left(V_B\right)\left(1 - \frac{\rho_B}{\rho_a}\right) + \left(A_B\right)\left(C_D\right)\left(1/2\ \rho_a\right)\left(\frac{dR}{dt}\right)^2 \quad \text{Eq (3)}$$

where

ρ_B Density of bubble

V_B - Volume of bubble

R Distance from center of rotation, + radially outward

t - Time

ω = Rotation rate

ρ_a - Density of cold, unburned gas

A_B = Projected area of bubble

C_D = Drag coefficient based on projected area.

Rearranging terms, equation 3 becomes:

$$\frac{d^2R}{dt^2} = -\left(\frac{R\omega^2}{\rho_B/\rho_a}\right)\left(1 - \rho_B/\rho_a\right) + \left(\frac{A_B C_D}{2\ V_B}\right)\left(\frac{\rho_a}{\rho_B}\right)\left(\frac{dR}{dt}\right)^2. \quad \text{Eq (4)}$$

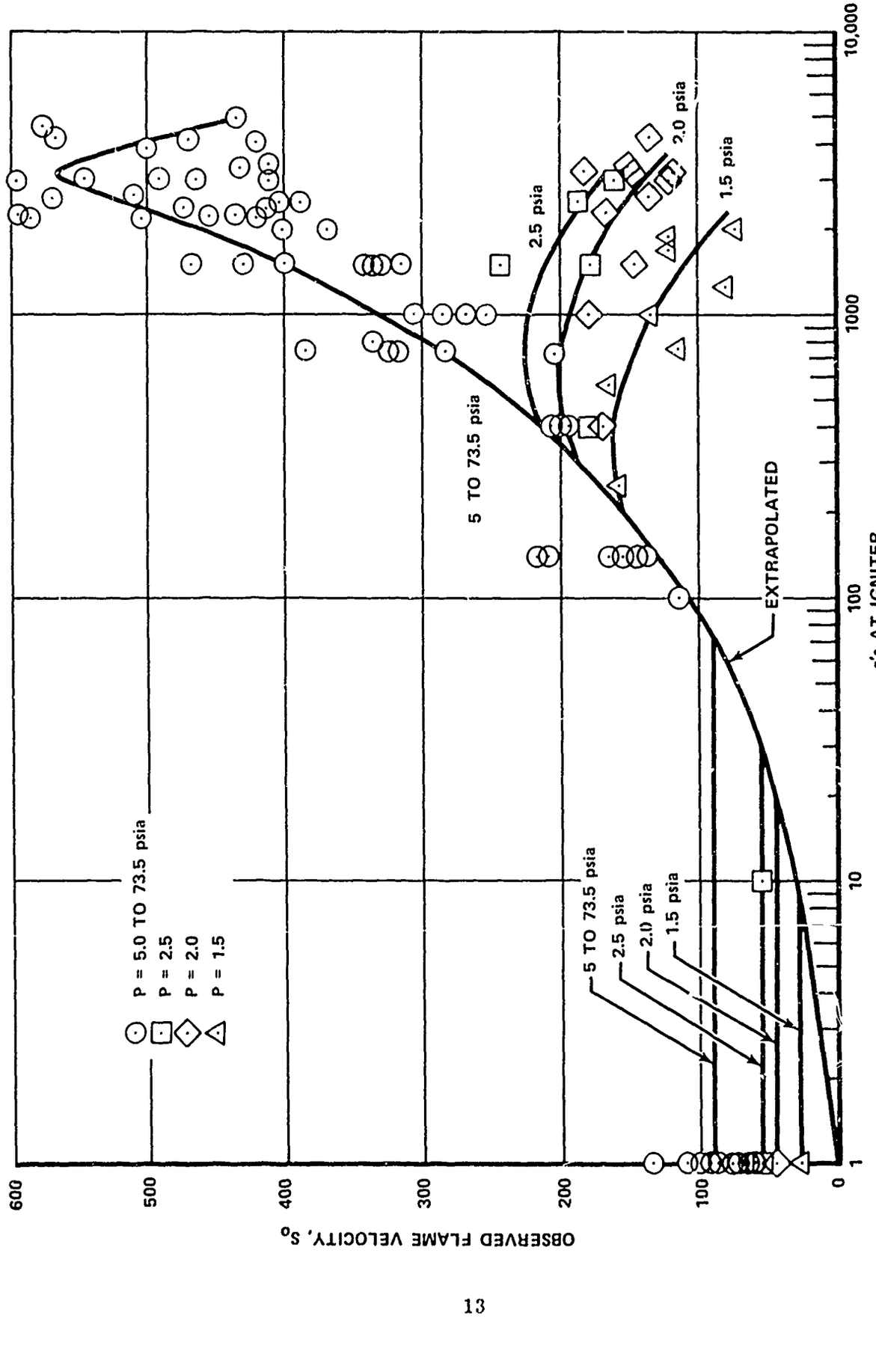

Figure 7. Pressure Effect on Flamespreading Rate for Propane–Air Mixtures, Φ - 0.8 to 1.4

FD 81455

If it is assumed that the flame rapidly accelerates to a terminal velocity where buoyant and drag forces are equal, d^2R/dt^2 becomes zero and the equation can be expressed as:

$$\left(\frac{dR}{dt}\right)^2 = S_B^2 = \left(1 - \frac{\rho_B}{\rho_a}\right)\left(R\omega^2\right)\left(\frac{A_B C_D}{2 V_B}\right). \qquad \text{Eq (5)}$$

Representing volume, V_B, divided by the projected area, A_B, by a characteristic length, L, and the centrifugal acceleration $R\omega^2$ by a, the equation further refines to:

$$S_B = \left[\left(\frac{2L}{C_D}\right)(a)\left(1 - \frac{\rho_B}{\rho_a}\right)\right]^{1/2}. \qquad \text{Eq (6)}$$

In a continuously flowing combustion system, however, such as a turbojet engine afterburner and in the combustion centrifuge, the bubble can not accelerate to terminal velocity within the confines of the combustion system and the assumption of a constant terminal velocity is not valid. In a flowing system, if the centrifugal force field is generated by swirling the air tangentially about the burner axis, the centrifugal acceleration varies with radius. In the combustion centrifuge, the centrifugal acceleration also varies with radius. Because of the difficulty in finding a closed solution to the differential equation, two, step-integration computer programs were formulated. One program represents a static system, such as the combustion centrifuge, and the second represents a flowing system, such as a turbojet augmentor. A description of the programs, sample results, flow diagrams, and computer listings is presented in Appendixes B and C.

In equation 4 all of the terms can be explicitly defined for a known gravitational field except the term $2V_B/A_BC_D$. A literature search was made to assist in defining this term. Data in the literature for air bubbles in liquid (Reference 1) and flame bubbles in a cold fuel-air mixture (Reference 2) show the same characteristic shape. The bubbles have a characteristically lenticular shape, with a spherical leading surface and a flat or slightly concave back surface. The shape is almost perfectly represented by a segment of a sphere, as shown in figure 8. In Reference 3 it was shown that air bubbles form this shape at Reynolds numbers over 4000, based on bubble diameter. A constant value of C_D is also

associated with these Reynolds numbers. This implies that a constant bubble half angle, θ_{max}, (figure 8) is maintained for bubbles with Reynolds numbers greater than 4000.

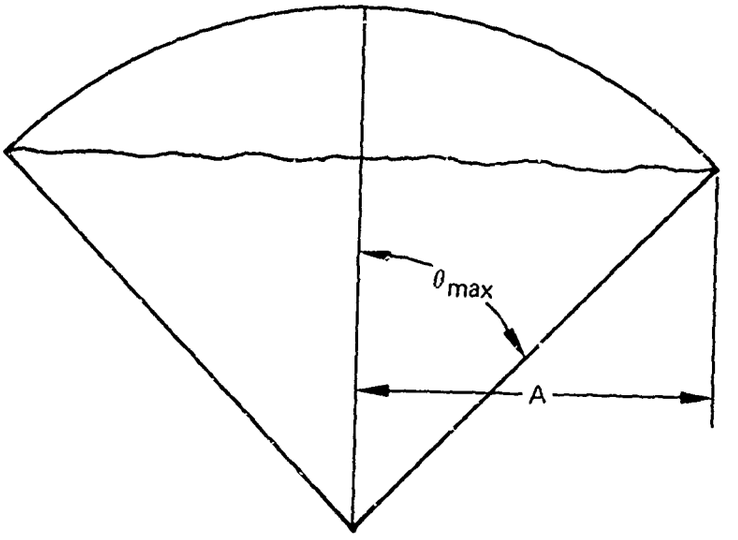

Figure 8. Details of Air or Flame Bubble FD 89698

The drag coefficient can be calculated by equating the drag force to the buoyant force on the bubble,

$$C_D \left(\frac{1}{2} \rho V^2 \pi A^2 \right) = V_B \rho g \qquad \text{Eq (7)}$$

where

C_D = Drag coefficient

ρ = Density of water

V = Velocity of bubble

V_B = Volume of bubble

g = Gravitational acceleration

A = Radius of bubble.

Rearranging terms,

$$C_D = \frac{V_B \, g}{0.5 \, V^2 \pi A^2} \, . \qquad \text{Eq (8)}$$

The velocity of the bubble can be calculated by using the theoretical model in Reference 1.

$$V = \frac{2}{3}\left(Ag/\sin\theta_{max}\right)^{1/2} \qquad \text{Eq (9)}$$

This equation was derived by holding the static pressure in Bernoulli's equation constant along the bubble surface. Experimental data have verified the model.

From geometric considerations, the volume of the bubble is

$$V_B = \frac{\pi A^3}{\sin^3\theta_{max}}\left[\frac{1}{3}\cos^3\theta_{max} - \cos\theta_{max} + \frac{2}{3}\right]. \qquad \text{Eq (10)}$$

Substituting velocity and volume into equation 8, it becomes

$$C_D = \frac{18}{4}\,\frac{\left[\frac{1}{3}\cos^3\theta_{max} - \cos\theta_{max} + \frac{2}{3}\right]}{\sin^2\theta_{max}}. \qquad \text{Eq (11)}$$

Taking $\theta_{max} = 46°$, $C_D = 0.728$. The term $2V_B/A_BC_D$ can now be calculated.

$$\frac{2V_B}{A_BC_D} = \frac{2\pi A^3}{\sin^3\theta_{max}}\,\frac{\left[\frac{1}{3}\cos^3\theta_{max} - \cos\theta_{max} + \frac{2}{3}\right]}{\pi A^2 C_D} \qquad \text{Eq (12)}$$

$$\frac{2V_B}{A_BC_D} = \frac{A}{1.618} \qquad \text{Eq (13)}$$

The term $2V_B/A_BC_D$ is a function of bubble radius A in an unconfined system. In a confined system, such as the combustion centrifuge, the same relationship holds, except the drag coefficient is larger because of pipe wall effects and therefore the constant (1.618) has a different value. From figure 9, which is a duplicate of figure 10 in Reference 4, the drag coefficient in the pipe can be roughly calculated to be 1.24 for a 1-inch radius bubble. The term $2V_B/A_BC_D$ equals 0.0303 for this drag coefficient. Using this value for $2V_B/A_BC_D$ in the flame bubble model discussed in Appendix B gave very good agreement with experimental data from the combustion centrifuge. Figure 10 compares the theoretical and experimental results.

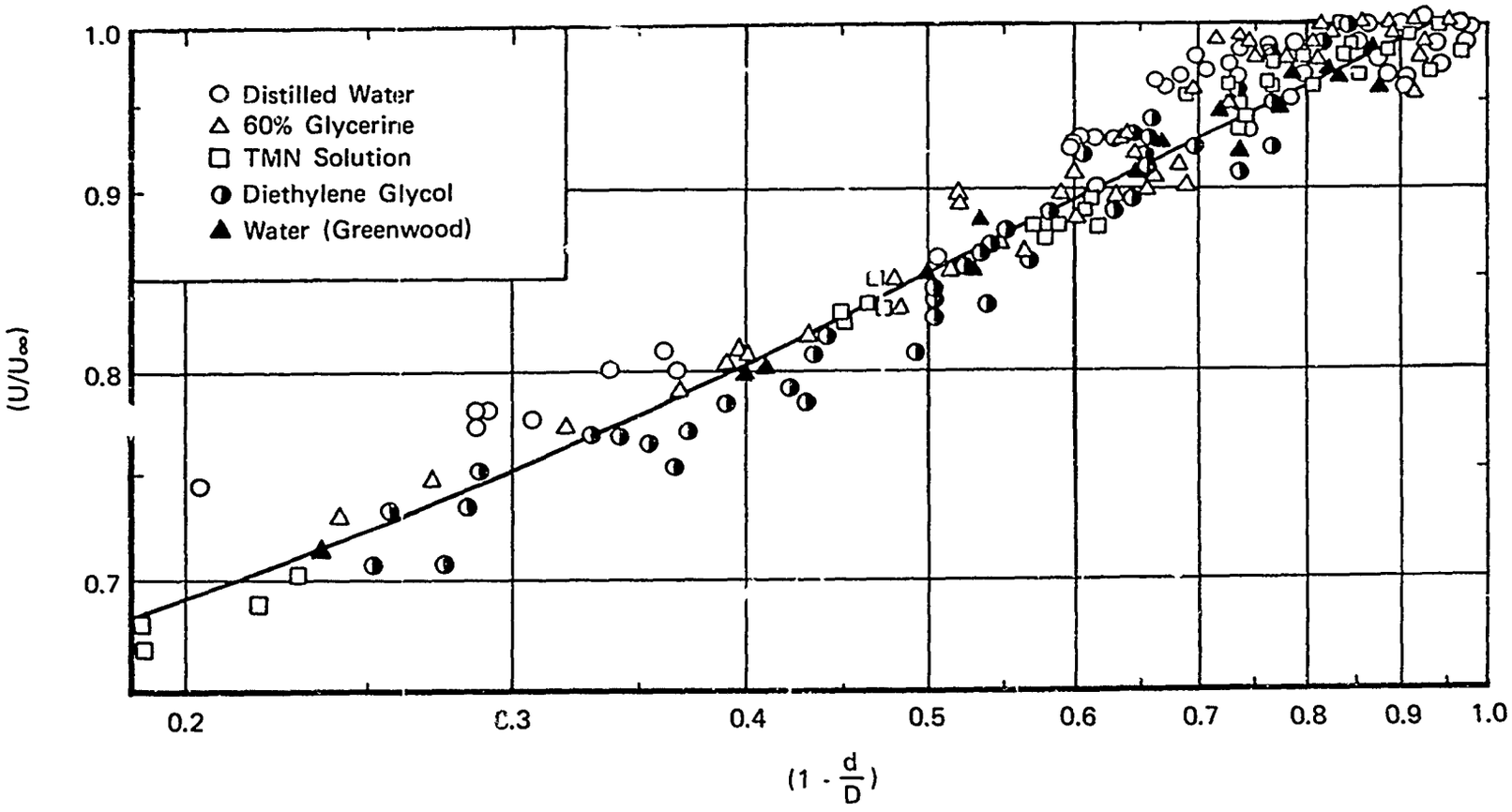

U = Bubble Velocity in Confined Space
U_∞ = Bubble Velocity in Unconfined Space
d = Bubble Diameter
D = Tube Diameter

Figure 9. Plot of Original Data as (U/U_∞) vs $(1-d/D)$

FD 89699

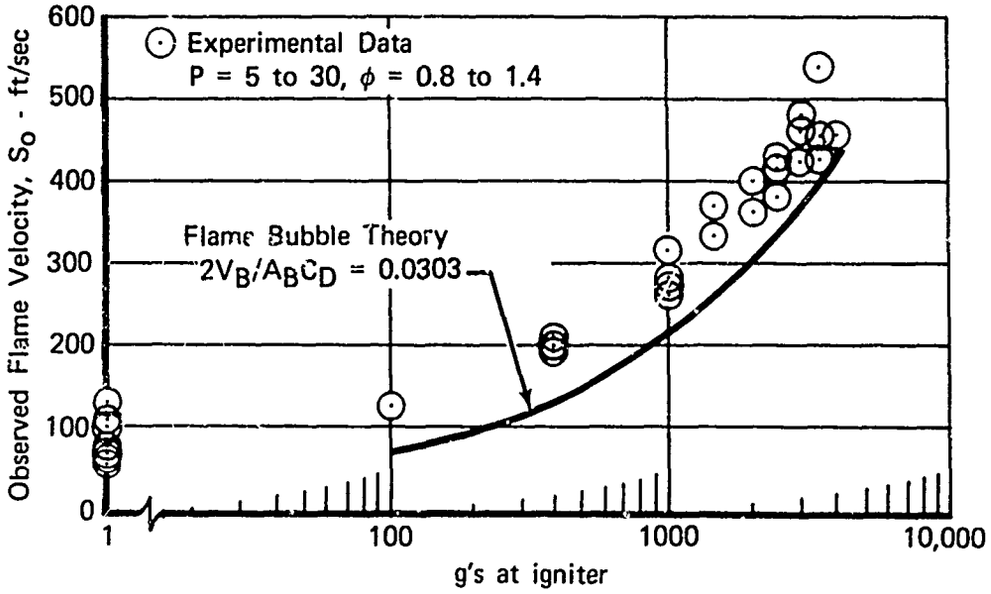

Figure 10. Theoretical vs Experimental Results in Combustion Centrifuge FD 89700

When reviewing the literature, it became apparent that there were no data available on air bubbles at very large Reynolds numbers. It is hypothesized that a limit Reynolds number is reached in which either the scale or intensity of turbulence becomes great enough to break the bubble apart. It was reported in Reference 5 that turbulent wakes behind air bubbles do occur. Therefore, the beginning of turbulence itself does not break the bubble and a higher Reynolds number is reached before bubble growth is limited by turbulence.

An experimental investigation was undertaken to determine the limiting Reynolds number. Single air bubbles of various sizes were released in sea water from a depth of 60 feet and photographed as they rose to the surface. (See figure 11.) Air bubbles enlarge as they rise because of the decrease in pressure, and their velocity (and Reynolds number) increase in proportion to their size. A bubble breakup always occurred when a limiting Reynolds number was reached. The experimental terminal velocity vs bubble Reynolds number is compared with theory in figure 12. The experimental data agree reasonably well with theoretical values.

Figure 11. Air Bubble Breakup FC 31384

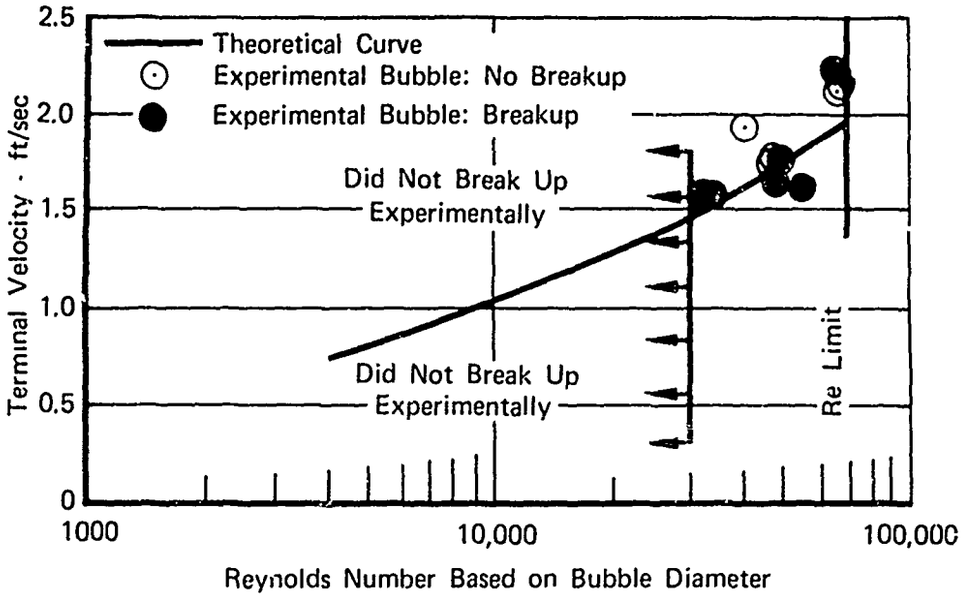

Figure 12. Terminal Velocity vs Reynolds Number for Air Bubbles Rising in Water FD 89701

The limiting Reynolds number was found to be equal to 70,000, based on bubble diameter. In relatively unconfined systems, such as large swirl combustion systems, the limiting Reynolds number is hypothesized to define the maximum bubble size if the Reynolds number of the bubble equals or exceeds 70,000. Otherwise, the bubble size depends on the pilot dimension.

2. Extinction Limits

The second area of investigation is the determination of the centrifugal force limit at which the flame is extinguished. Because the combustion centrifuge is limited by structural considerations to speeds producing less than 5000 g, it was not possible directly to measure the limiting g value over most of the fuel-air ratio range. However, at very lean and very rich fuel-air ratios, the limiting centrifugal force values fell within the centrifuge operating range. At these conditions the limit was extremely sensitive to small variations in fuel-air ratio and temperature, and, as a result, the data are somewhat scattered. Tests from a single mixture of fuel and air generally gave very consistent results, but tests using another batch mixed to the same specifications (±2%) often produced a parallel but displaced line of data. Typical results for nominal 0.0375 and 0.045 fuel-air ratios are presented in figure 13. As shown in the figure, there appear

to be three different extinction mechanisms controlling different regimes of operation. At the bottoms of the two lines of data, there is a low pressure limit below which flame will not propagate regardless of the centrifugal force. This pressure limit is the same with the centrifuge stationary and with it operating to produce the g values indicated on the figures. It is believed that this limit is established by flame-quenching in the holes of the turbulence generator and is not pertinent to this investigation. Above this low pressure limit and below about one atmosphere, a second mechanism controls the flame extinction limits. In this region, increasing pressure permits operation to increasingly higher centrifugal force values. It is postulated that this is a regime where viscosity effects are sufficiently strong relative to density differences so that true flame bubbles controlled by buoyant forces do not become organized before the turbulence created by their organization cools and quenches the flame. In the major regime of operation, above one atmosphere pressure, the experimental data are relatively consistent and agree quite well with the results predicted by the following analytical model.

a. Analytical Extinction Model

Figure 14 represents a flame bubble rising through a cool mixture of fuel and air under the influence of buoyant forces. The heat generated in the bubble can be expressed as the heat of combustion (ΔH) multiplied by the mass of fuel-air mixture burned. This, in turn, can be expressed as the density (ρ_a) multiplied by the laminar flamespeed (Su) and the instantaneous area of the bubble (A).

$$Q_{in} = (\Delta H)\ (\rho_a)\ (Su)\ (A) \qquad \text{Eq (14)}$$

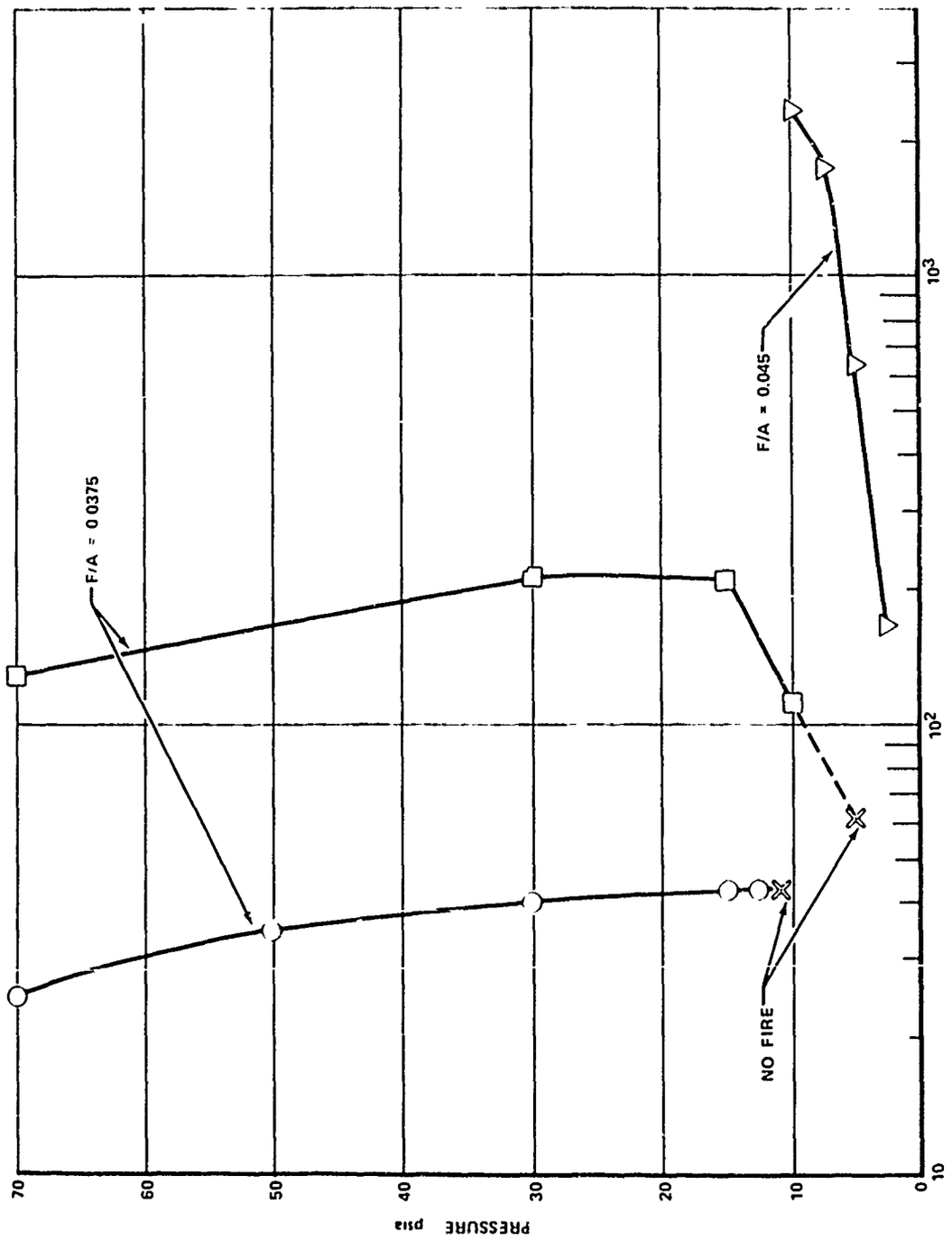

Figure 13. Limiting Centrifugal Acceleration as a Function of Pressure

FD 81456

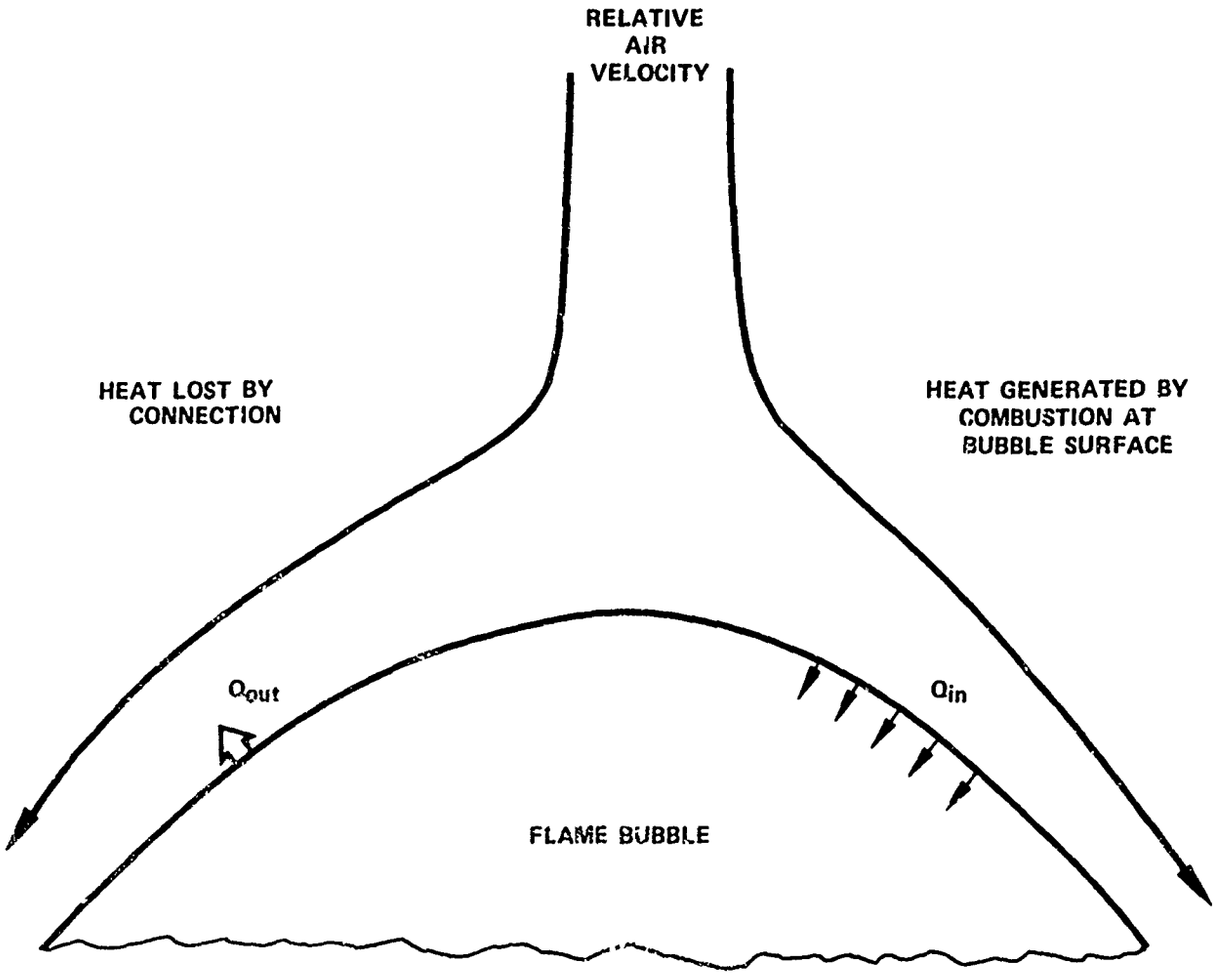

Figure 14. Schematic Representation of Flame Bubble Heat Generation and Loss FD 81457

The heat lost from the bubble, neglecting radiation, can be approximated by the classical equation for convective heat transfer,

$$Q_{out} = (h)\ (A)\ (\Delta T) \qquad \text{Eq (15)}$$

where h is the convective heat transfer coefficient, A is the heat transfer surface area, and ΔT is the temperature difference between the bubble flame temperature and the surrounding fuel-air mixture temperature. The convective heat transfer coefficient, in turn, can be evaluated from

$$\text{Nusselt No.} \quad \left(C_1\right)(\text{Reynolds No.})^{0.8}\ (\text{Prandtl No.})^{0.4} \qquad \text{Eq (16)}$$

where C_1 is an empirical constant. From this relationship,

$$Q_{out} = \left(\frac{K}{D}\right)\left(C_1\right)\ (A)\ (Re)^{0.8}\ (Pr)^{0.4}\ (\Delta T) \qquad \text{Eq (17)}$$

where K is thermal conductivity and D is flame bubble diameter.

At the point where fire is extinguished, the rate of heat generation must equal the rate of heat loss,

$$Q_{in} = Q_{out} \qquad \text{Eq (18)}$$

or

$$(\Delta H)\ (\rho_a)\ (Su)\ (A) = \left(\frac{K}{D}\right)\left(C_1\right)\ (A)\ (Re)^{0.8}\ (Pr)^{0.4}\ (\Delta T). \qquad \text{Eq (19)}$$

If the velocity term in the Reynolds No. is taken as the bubble velocity expressed in equation 6, the equation can be solved for g as shown below:

$$g = C_2\left\{\left[\frac{1}{\sqrt{1-\frac{\rho_B}{\rho_a}}}\right]\left[\frac{\mu}{D\rho_a}\right]\left[\frac{(Su)\ (\rho_a)\ (\Delta H)\ (D)}{(\Delta T)\ (Pr)^{0.4}\ (K)}\right]^{1.25}\right\} \qquad \text{Eq (20)}$$

where μ is viscosity, and C_2 is a constant that includes C_1 and provides consistent units.

Solving this equation using physical properties based on the cold fuel-air mixture and selecting D as 90% of the centrifuge pipe diameter (based on photographs in Reference 1) results in the predicted extinction limits presented in figure 15. Very good agreement with the experimental data is evident. It is interesting to note that, in addition to conversion factors to provide compatible units, the constant C_2, 4.15×10^{14} in equation 20, also contains constant C_1 (from equation 16). The constant C_1 needed to obtain this agreement of experimental data and analytical predictions is 0.0535, compared to the conventional 0.023 used for heat transfer between a fluid and a solid pipe surface.

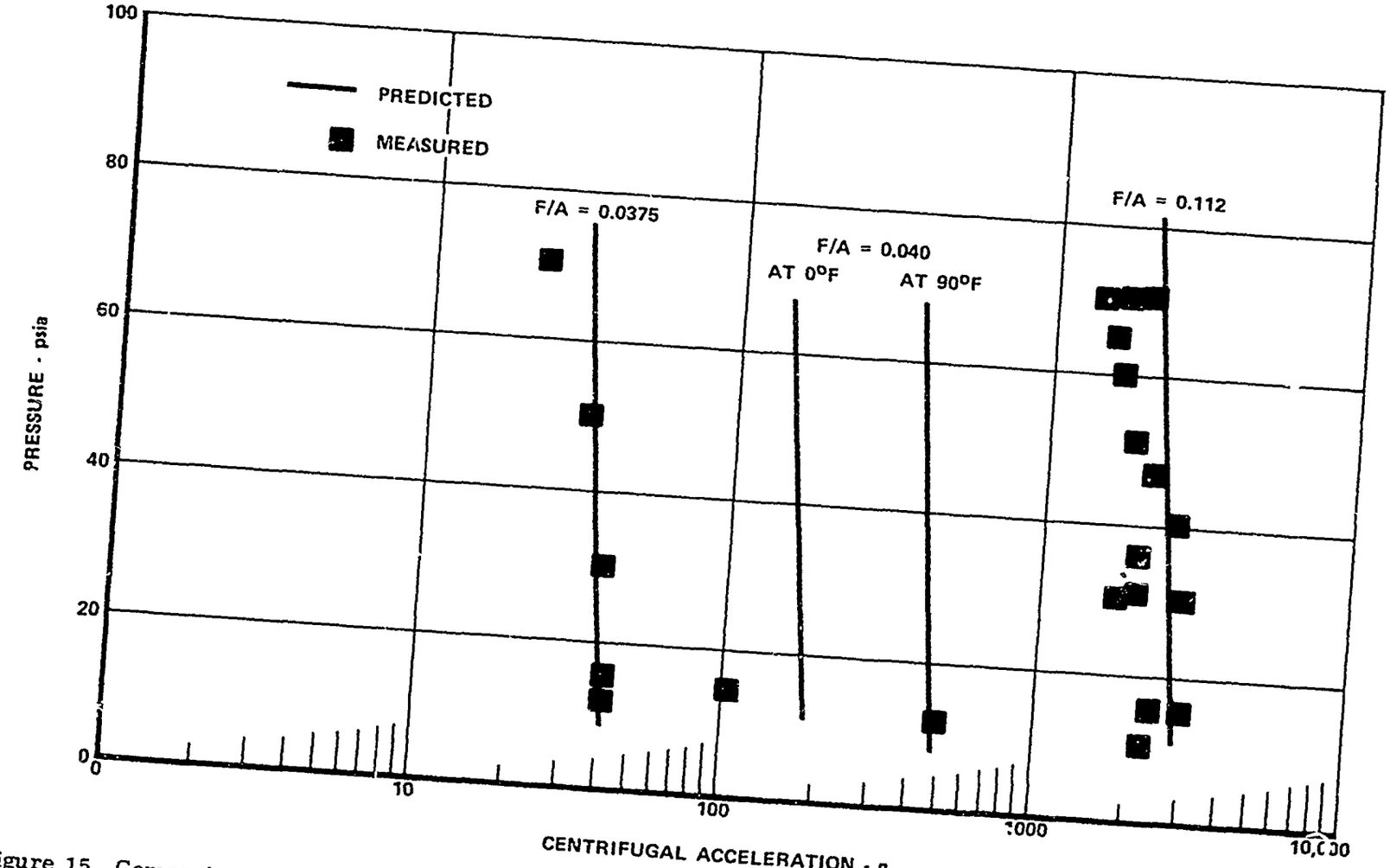

Figure 15. Comparison of Predicted and Measured Flame Extinction Limits

FD 81458

Because of the ability to predict flame extinction from a cooling analysis, changing only the empirical constant, it appears that this approach may also have merit in predicting blowoff from conventional flameholders.

3. Reynolds Number Effects

Another area of investigation involves the effects of Reynolds No. on turbulent flamespeed in gravitational fields low enough so that buoyancy has no effect on flame propagation rates. The rate of flame propagation and flamefront shape were measured with ionization probes while hydrogen-air or propane-air mixtures were burned in polyvinyl chloride pipes of three different diameters. The apparatus is shown in figure 16. Each tube contained a sparkplug located behind a turbulence generator to ensure the rapid generation of a turbulent flame. Two ionization probes detected the passage of the center of the flamefront at a point 12 inches downstream of the turbulence generator, and a second set of probes detected the passage of the flame at five radial positions in a plane 12 inches downstream of the first set. Thus, the two sets of probes provided measurements of both the average speed between the two sets and the shape of the flamefront at the second set.

To conduct a test, a plate and a paper disk were placed over the open end of the PVC tube (which was coated with vacuum grease), and a vacuum was pulled to remove all air, moisture, and products of prior combustion from the rig. The previously prepared fuel-air mixture was then admitted to the pipe from a separate premixed supply tank until atmospheric pressure was reached. The metal disk was then slipped off, and the paper disk was left adhering to the vacuum grease. The sparkplug was then fired, and the flame passage was recorded at essentially constant atmospheric pressure.

The observed flamespeed was the sum of the turbulent flamespeed plus the velocity of the cold mixture due to the expansion caused by combustion in the closed end of the pipe. If the flamefront is a flat plane and there is no inefficiency or heat loss, the turbulent flamespeed can be approximated from the expression,

$$S_T \quad \frac{U_o}{T_2/T_1} \qquad \text{Eq (21)}$$

where S_T is turbulent flamespeed, U_o is the observed velocity, and T_1 and T_2 are temperatures before and after combustion. This equation also assumes the number

of moles before and after combustion are nearly the same. This is correct within 4% for stoichiometric or leaner propane-air mixtures, but a correction for the almost 15% change in number of moles was required for the hydrogen-air mixtures.

Figure 16. Tubes Used To Measure Reynolds Number Influence on Flamespeed FE 336140

If the flamefront is not a flat plane, equation 21 can be corrected for the measured flamefront area as shown below:

$$S_T = \frac{U_o}{1 + \left(\frac{A_1}{A_2}\right)\left(\frac{T_2}{T_1} - 1\right)} \qquad \text{Eq (22)}$$

where A_1 is the flamefront area and A_2 is the pipe cross-sectional area.

In most of the experiments conducted A_1/A_2 was so close to 1.0 that it could be neglected. Typical flamefront profiles for hydrogen-air and propane-air mixtures are presented in figure 17.

Using equation 22 to calculate the turbulent flamespeed, taking the laminar flamespeed from the literature, and calculating Reynolds No. from the cold gas velocity ($U_o - S_T$) resulted in the data shown in figure 18. The turbulent-to-laminar flamespeed ratio increases rapidly as turbulence increases until a maximum is reached. Beyond that point the flame is stretched so thin that some of it is cooled to extinction, and further increase in turbulence results in a decrease in turbulent flamespeed. It is significant that both propane-air mixtures with a stoichiometric laminar flamespeed of 1.3 feet per second and hydrogen-air mixtures with a stoichiometric laminar flamespeed of 6.2 feet per second fit the same curve.

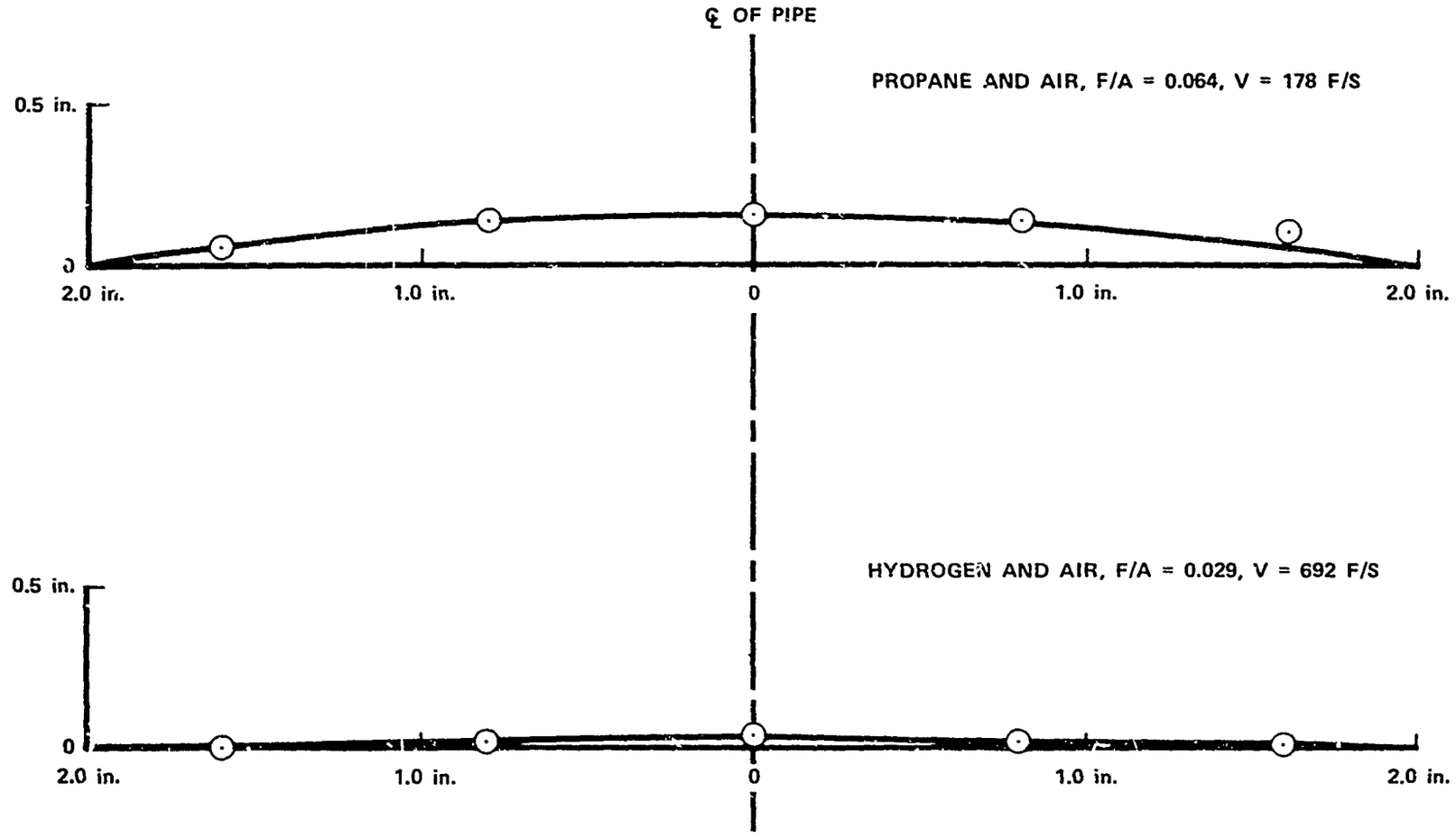

Figure 17. Shape of Flamefront in PVC Pipes

FD 81459

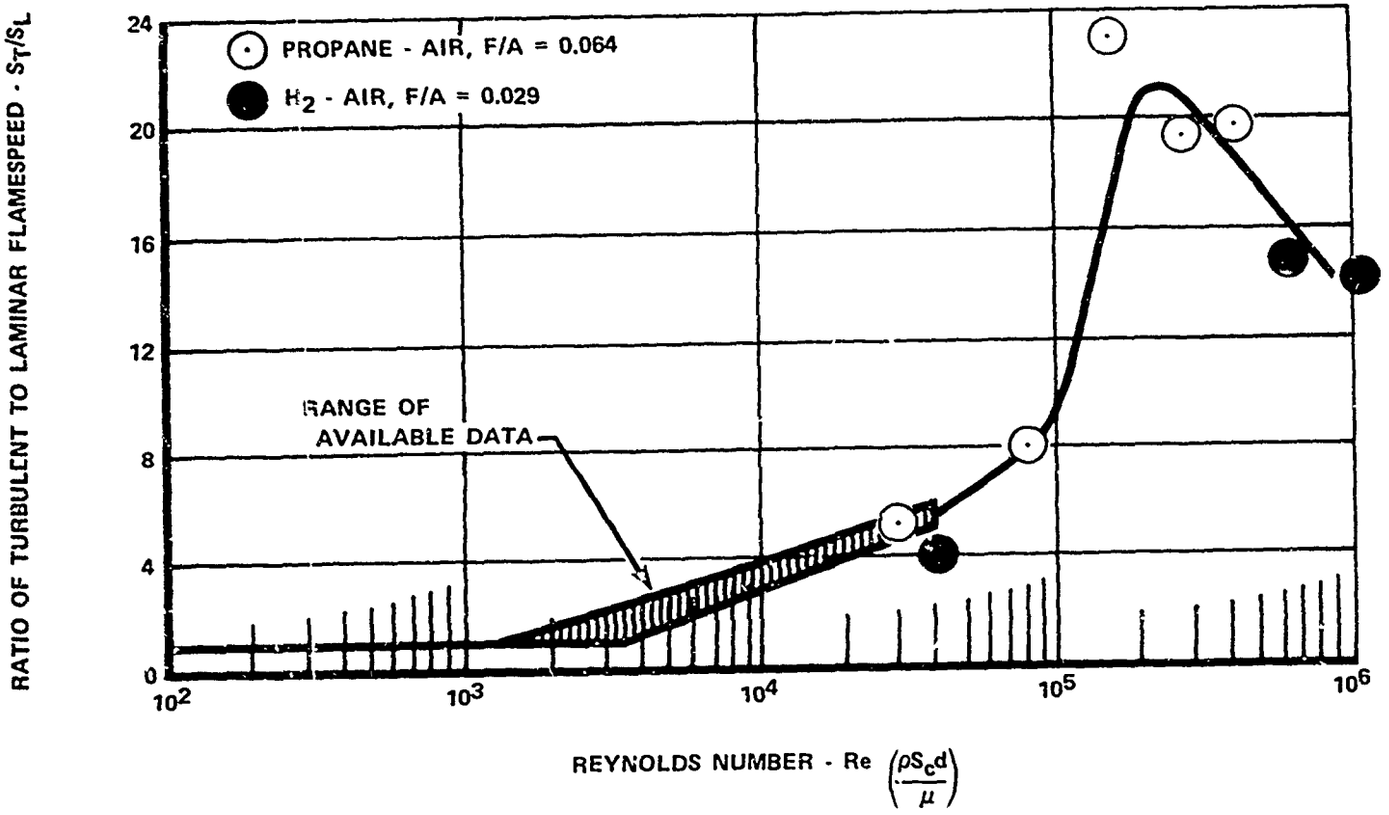

Figure 18. Ratio of Turbulent to Laminar Flamespeed as a Function of Reynolds Number

FD 81460

4. Application of Results

The end objective of all research work is the practical application of the research results. One practical application of the increased flamespeed resulting from centrifugal effects is the swirl augmentor. Augmentors are currently used in aircraft turbojet and turbofan engines to provide thrust augmentation. Conventional augmentors use numerous flameholders, which act as ignition sources to burn the flowing fuel-air mixture (figure 19). Large pressure losses (4%) and long augmentor lengths ($L/D \approx 2.5$) are associated with conventional augmentors. As an alternative, the swirl augmentor has been proposed. Swirl augmentors use precombustion swirl vanes to swirl the flow and produce a centrifugal field that increases the burning rate of the combustible mixture. In figure 20 a schematic of a swirl augmentor tested under another program is presented to define the essential details. Fuel is inserted into the swirling flow by sprayrings, and the combustible mixture is ignited by a circumferential pilot on the outer wall of the combustion duct. Initiating at the pilot, the flame bubbles move quickly to the center due to the buoyant effect of the hot burned gases in the cold unburned gases, igniting the fuel-air mixture as they go. Since the bubble speed can be many times greater than turbulent flamespeed in conventional augmentors, shorter lengths or higher burning efficiencies result. Pressure losses are less than with conventional augmentors, especially if movable vanes are used which are set to zero degrees during non-augmented flight. In addition, the swirl augmentor has the added performance advantage of being unaffected by pressure and Mach number changes.

To permit practical application of these principles, a swirl combustor design system has been developed, evaluated, and applied. Details of the design system and a computer listing are presented in Appendix C.

The model's prediction of radial flame movement is based on equation 4 and radial expansion of the burned gases. Axial movement is calculated from the initial axial gas velocity increased by the expansion resulting from combustion. The result is a flamefront profile (similar to that in figure 20), which is a function of design variables.

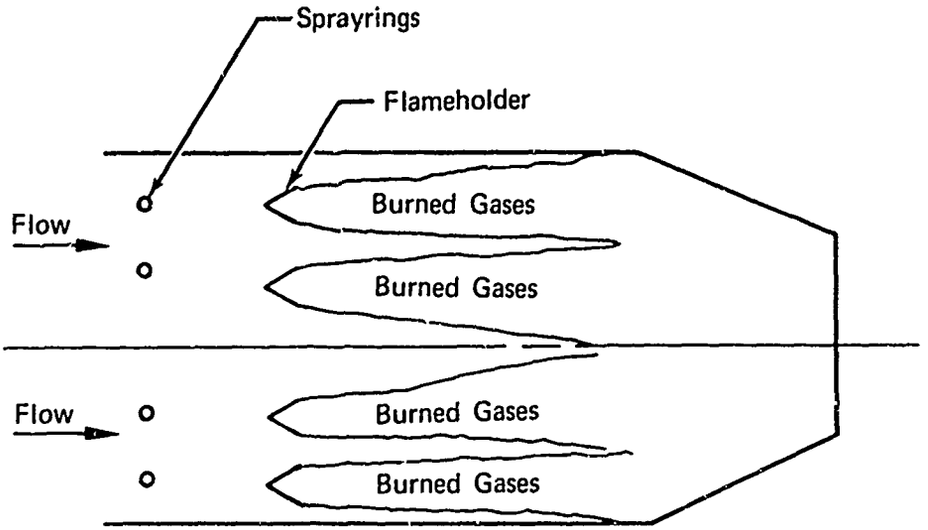

Figure 19. Schematic of a Conventional Augmentor FD 89702

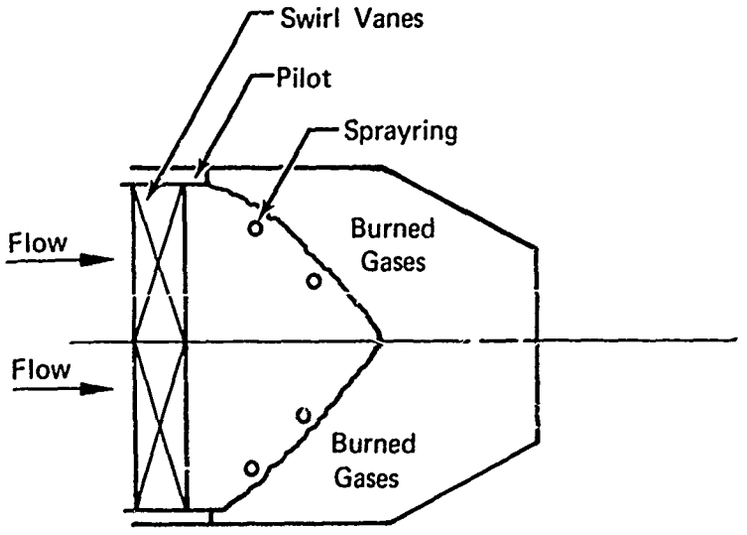

Figure 20. Schematic of a Swirl Augmentor FD 89703

The model was used to predict the combustion efficiency as a function of length for a 15-inch diameter swirl augmentor rig, which was tested under another program. Unfortunately, the maximum bubble Reynolds number was not reached in this small rig. In order to predict flamespreading rates, a bubble diameter was selected equal to the pilot dimension. A comparison of the predicted and experimental results is presented in figure 21. After this verification of the model, it was used to design a swirl augmentor for an advanced version of a large Air Force turbofan engine. This design is presented in figure 22. The reduced pressure loss and reduced sensitivity of the swirl augmentor to augmentor pressure and gas velocity are predicted to produce a 2% reduction in fuel consumption and to increase stability at high-altitude, low-Mach-number flight conditions. For this application, the augmentor length was not changed from that of the current engine, and the benefit was taken as reduced pressure loss and fuel consumption. Alternatively, the pressure loss could have been held constant and the benefits of reduced length and weight would have resulted, as shown in figure 23.

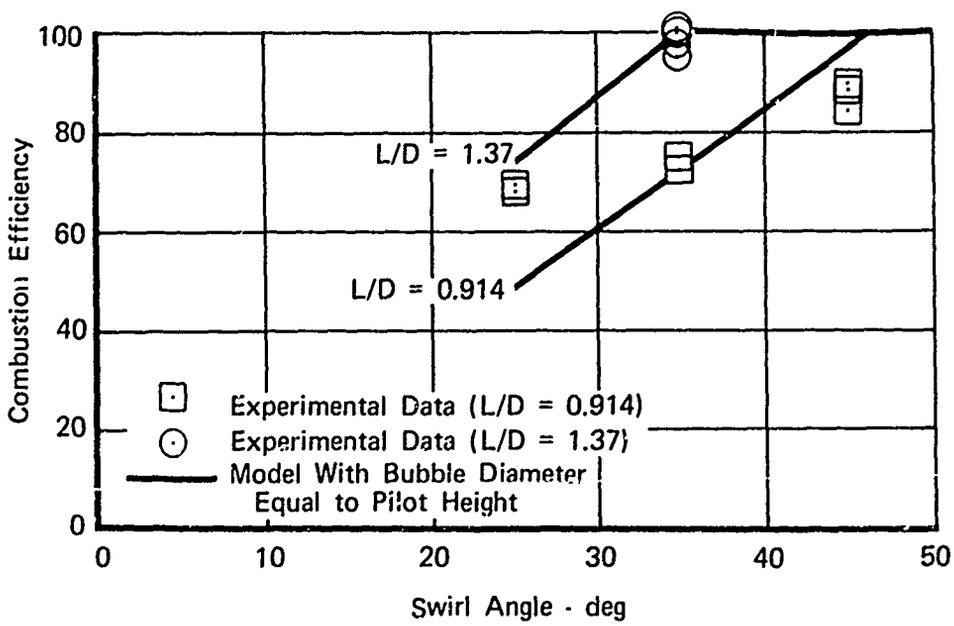

Figure 21. Comparison of Experimental and Theoretical Results at Augmentor Equivalence Ratios Between 0.95 and 1.05

FD 89704

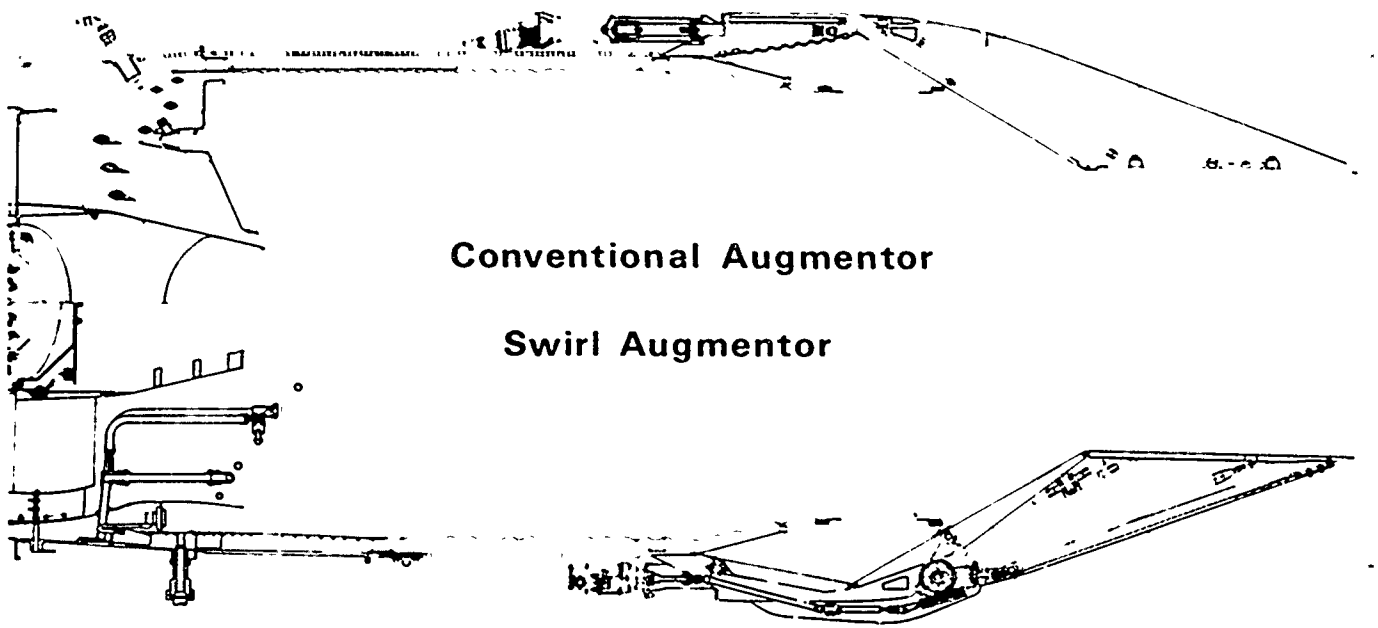

Figure 22. Comparison of a Conventional Augmentor and a Swirl Augmentor in a Large Air Force Turbofan Engine FD 85510

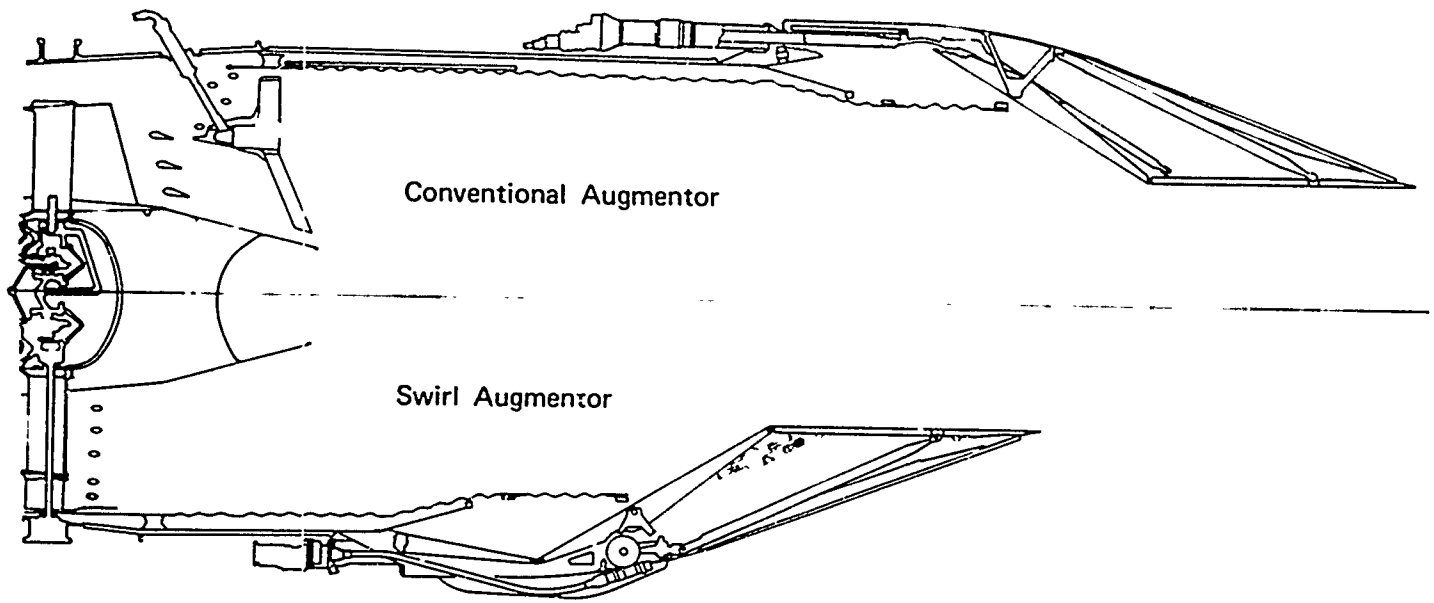

Figure 23. Reduced Length Design Version of Swirl Augmentor in a Large Air Force Turbofan Engine FD 27658

Another application in which the model was used was in sizing a ramburner system for an advanced high-Mach aircraft demonstrator propulsion system. Since size and weight were at a premium for this application, every effort was made to minimize both of those parameters. As shown in figure 24, the swirl ramburner was designed using the model and is significantly smaller in size and also weight when compared to the more conventional preburner-ramburner. Both of the ramburner systems were sized for the same thrust.

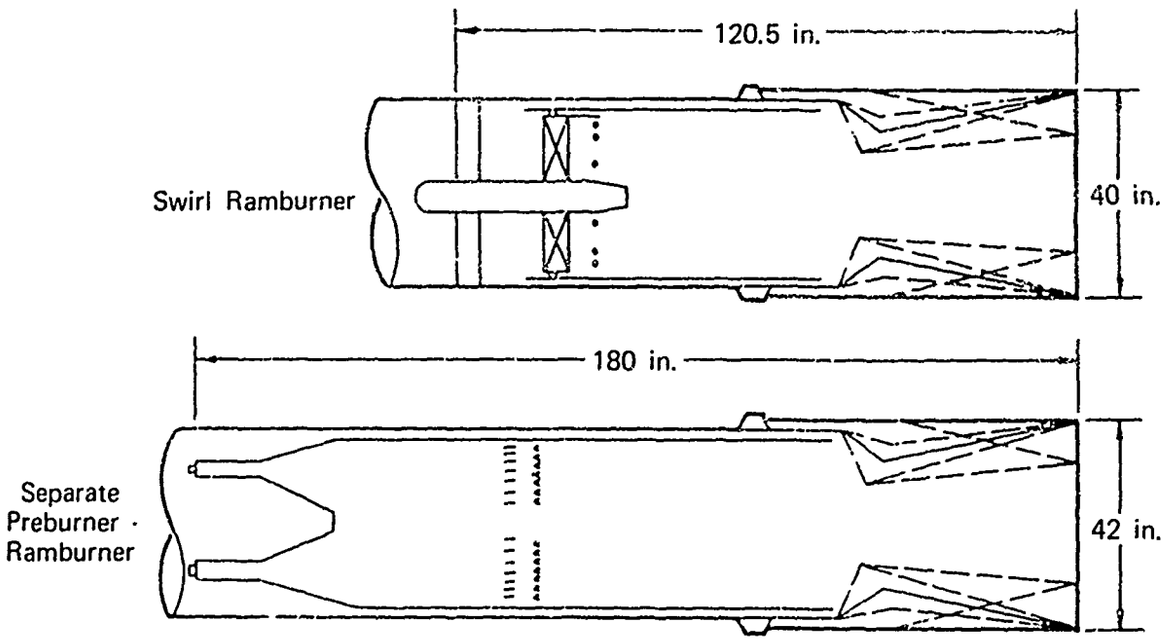

Figure 24. Swirl Burner Concept Reduces Ramburner Length - Ramburners Sized for the Same Thrust FD 90740

SECTION III
CONCLUSIONS

1. A bubble theory of flame propagation has been developed and can be successfully used to design swirl flow combustion systems.

2. A theory has been developed that predicts with reasonable accuracy the extinction limits of a flame in a high centrifugal force field.

3. The turbulent flamespeed of a fuel-air mixture increases with increasing Reynolds number, until a maximum is reached beyond which flame stretch quenches flame ligaments and results in lower turbulent flamespeeds.

APPENDIX A
EXPERIMENTAL DATA

Table A-1. Centrifuge Test Conditions for Propane and Air

Run	f/a	Pressure, psia	Temperature, °F	rpm
1	0.064	15	Unrecorded	0
2	0.064	15	Unrecorded	0
3	0.064	15	Unrecorded	850
4	0.064	15	Unrecorded	0
5	0.064	15	Unrecorded	0
6	0.064	15	Unrecorded	0
7	0.064	15	Unrecorded	850
8	0.064	15	Unrecorded	850
9	0.064	15	Unrecorded	2,015
10	0.064	15	Unrecorded	1,722
11	0.064	15	Unrecorded	1,570
12	0.064	15	Unrecorded	1,404
13	0.064	15	Unrecorded	1,212
14	0.064	15	Unrecorded	990
15	0.064	15	Unrecorded	625
16	0.089	15	Unrecorded	0
17	0.089	15	Unrecorded	993
18	0.089	15	83	1,409
19	0.089	15	83	1,567
20	0.089	15	98	0
21	0.089	15	99	1,710
22	0.089	15	Unrecorded	1,820
23	0.089	15	103	316
24	0.089	30	103	0
25	0.089	30	100	627
26	0.089	30	98	990
27	0.089	30	98	1,813
28	0.089	5	98	1,797
29	0.089	2	98	1,790
30	0.089	1	103	1,491
31	0.089	1	97	0
32	0.089	1	98	402
33	0.089	1	100	451
34	0.089	1	100	0
35	0.089	1	102	0
36	0.089	1	104	504
37	0.089	1	104	0
38	0.089	2	104	1,000
39	0.089	2	104	1,507
40	0.089	2	103	1,602
41	0.089	2	106	1,768
42	0.089	2	106	1,765
43	0.089	1.5	103	1,402
44	0.089	1.5	104	1,369
45	0.089	1.5	104	1,298

Table A-1. Centrifuge Test Conditions for Propane and Air (Continued)

Run	f/a	Pressure, psia	Temperature, °F	rpm
46	0.089	1.5	101	0
47	0.089	1.5	102	490
48	0.089	1.5	104	746
49	0.089	1.5	105	876
50	0.089	1.5	106	1,000
51	0.089	1.5	106	1,102
100	0.064	2.5	Unrecorded	0
101	0.064	2.5	Unrecorded	0
102	0.064	5.0	Unrecorded	0
103	0.064	2.5	Unrecorded	1,200
104	0.064	5.0	Unrecorded	0
105	0.064	5.0	Unrecorded	101
106	0.064	5.0	Unrecorded	625
107	0.064	5.0	Unrecorded	1,210
108	0.064	5.0	Unrecorded	1,565
109	0.064	5.0	Unrecorded	990
110	0.064	5.0	Unrecorded	1,714
111	0.064	2.5	Unrecorded	625
112	0.064	2.5	Unrecorded	1,209
113	0.064	2.5	Unrecorded	1,706
114	0.064	2.5	Unrecorded	100
115	0.064	2.5	Unrecorded	1,571
116	0.089	2	Unrecorded	0
117	0.089	2	Unrecorded	625
118	0.089	2	Unrecorded	1,210
119	0.089	2	Unrecorded	1,800
120	0.089	2	Unrecorded	2,000
121	0.089	2	Unrecorded	1,800
122	0.089	2	Unrecorded	1,700
123	0.089	2	Unrecorded	0
124	0.099	5	Unrecorded	C
125	0.099	5	Unrecorded	625
126	0.099	5	105	1,980
127	0.099	5	103	1,993
128	0.099	5	107	1,880
129	0.099	5	107	0
130	0.099	5	103	1,936
131	0.099	5	Unrecorded	0
132	0.099	5	105	2,000
133	0.099	5	Unrecorded	2,000
134	0.099	30	100	0
135	0.099	5	Unrecorded	2,100
136	0.099	5	Unrecorded	2,000
137	0.099	10	Unrecorded	2,100
138	0.099	10	Unrecorded	2,150
139	0.099	10	Unrecorded	2,150
140	0.099	15	Unrecorded	2,100
141	0.099	15	Unrecorded	2,100

Table A-1. Centrifuge Test Conditions for Propane and Air (Continued)

Run	f/a	Pressure, psia	Temperature, °F	rpm
142	0.099	15	Unrecorded	2,250
143	0.099	15	Unrecorded	2,308
144	0.099	5	Unrecorded	2,250
145	0.099	30	Unrecorded	2,100
146	0.105	15	Unrecorded	0
147	0.105	15	Unrecorded	1,600
157	0.112	15	105	0
163	0.112	5	Unrecorded	1,200
252	0.064	15	95	500
258	0.064	15	95	1,048
259	0.064	5	90	500
265	0.064	5	103	500
266	0.064	30	108	1,500
267	0.064	30	106	2,100
270	0.064	20	108	1,900
272	0.064	15	113	1,100
273	0.064	15	113	1,250
274	0.064	15	113	1,300
275	0.064	15	115	1,350
276	0.064	10	115	865
277	0.064	10	103	900
278	0.064	2.5	115	420
279	0.064	2.5	116	375
280	0.090	15	105	500
283	0.090	15	115	750
285	0.090	30	114	1,500
287	0.090	30	108	1,750
288	0.090	2.5	110	240
289	0.090	2.5	113	255
290	0.090	2.5	118	277
291	0.090	2.5	114	300
292	0.090	2.5	118	320
295	0.090	10	118	510
296	0.090	5	125	340
298	0.090	5	108	360
305	0.052	22.5	110	250
306	0.052	22.5	110	275
307	0.052	22.5	110	350
309	0.052	22.5	110	400
310	0.052	22.5	110	450
315	0.052	10	110	260
316	0.052	10	115	312
317	0.052	10	115	360
319	0.052	10	115	400
324	0.052	5	110	360
326	0.052	2.5	115	306
329	0.058	10	110	550
336	0.058	2.5	95	350

Table A-1. Centrifuge Test Conditions for Propane and Air (Continued)

Run	f/a	Pressure, psia	Temperature, °F	rpm
338	0.061	5	90	462
362	0.064	10	110	700
363	0.064	10	110	750
364	0.064	10	100	775
374	0.064	20	90	0
376	0.064	20	90	1,200
377	0.101	15	95	225
382	0.101	15	95	195
384	0.101	15	85	195
387	0.101	30	85	310
389	0.101	5	85	121
390	0.101	4.8	85	125
391	0.101	4.8	85	150
392	0.101	4.8	85	200
395	0.101	4.7	100	190
399	0.101	20	110	290
400	0.101	20	115	315
401	0.101	20	110	327
403	0.101	30	115	439
404	0.101	30	115	460
405	0.101	30	115	505
406	0.101	30	120	550
407	0.101	28.3	120	550
408	0.101	20	120	330

Table A-2. Centrifuge

Run	Probe Ft From Center	Time Sec After Spark	Probe Ft From Center	Time Sec After Spark	Probe Ft From Center	Tim Sec After
1	2.416	0.01676	2.333	0.01756	2.000	0.02
2	2.416	0.01627	2.333	0.01711	2.000	0.02
4	2.416	0.01579	2.333	0.01665	2.000	0.01
5	2.416	0.01634	2.333	0.01707	2.000	0.02
6	2.416	0.01699	2.333	0.01765	2.000	0.02
7	2.416	0.02005	2.000	0.02518	1.916	0.02
9	2.416	0.00468	2.000	0.00678	1.916	0.00
10	2.416	0.00669	2.000	0.00810	1.916	0.00
11	2.416	0.00681	2.000	0.00831	1.916	0.00
12	2.416	0.00760	2.000	0.00922	1.916	0.00
13	2.416	0.00805	2.000	0.00994	1.916	0.01
14	2.416	0.00909	2.000	0.00140	1.916	0.01
15	2.416	0.01138	2.000	0.01449	1.916	0.01
16	2.416	0.01423	2.000	0.01768	1.916	0.01
17	2.416	0.00841	2.000	0.01061	1.916	0.01
18	2.416	0.00729	2.000	0.00898	1.916	0.00
19	2.416	0.00721	2.000	0.00861	1.916	0.00
20	2.416	0.01550	2.000	0.01957	1.916	0.02
21	2.416	0.00630	2.000	0.00769	1.916	0.00
22	2.416	0.00652	2.000	0.00786	1.916	0.00
23	2.000	0.02055	1.916	0.02141	1.583	0.02
24	2.416	0.02092	2.250	0.02276	2.000	0.02
25	2.416	0.01352	2.250	0.01406	2.000	0.01
26	2.416	0.00835	2.250	0.00933	2.000	0.01
27	2.250	0.00639	2.000	0.00710	1.916	0.00
28	2.416	0.00552	2.250	0.00638	2.000	0.00
29	2.416	0.00656	2.250	0.00803	2.000	0.00
30	2.416	0.01006	2.250	0.01387	2.000	0.01
31	2.416	0.02767	2.250	0.03307	2.000	0.03
32	2.416	0.01957	2.250	0.02798	2.000	0.03
33	2.416	0.01964	2.250	0.02711	2.000	0.03
34	2.416	0.08446	2.250	0.11286	2.000	0.12
36	2.416	0.01756	2.250	0.02232	2.000	0.02
37	2.416	0.03054	2.250	0.03643	2.000	0.04
38	2.416	0.01076	2.250	0.01233	2.000	0.01
39	2.416	0.00914	2.250	0.01109	2.000	0.01
40	2.416	0.00850	2.250	0.01383	2.000	0.01
41	2.416	0.00626	2.250	0.00790	2.000	0.01
42	2.416	0.00838	2.250	0.01089	2.000	0.01
43	2.416	0.01095	2.250	0.01500	2.000	0.01
44	2.416	0.01042	2.250	0.01349	2.000	0.01
45	2.416	0.01041	2.250	0.01367	2.000	0.01
46	2.416	0.02108	2.250	0.02401	2.000	0.03
47	2.416	0.01538	2.250	0.01763	2.000	0.01
48	2.416	0.01231	2.250	0.01428	2.000	0.01
49	2.416	0.01170	2.250	0.01455	2.000	0.01
50	2.416	0.01253	2.250	0.01485	2.000	0.01
51	2.416	0.01413	2.250	0.01850	2.000	0.02
100	2.416	0.01518	2.250	0.01738	2.000	0.02

Table A-2. Centrifuge Test Data for Propane and Air

Probe om Center	Time Sec After Spark	Probe Ft From Center	Time Sec After Spark	Probe Ft From Center	Time Sec After Spark	Probe Ft From Ce
.000	0.02085	1.916	0.02185	1.583	0.02585	1.500
.000	0.02060	1.916	0.02175	1.583	0.02693	1.500
.000	0.01982	1.916	0.02067	1.583	0.02537	1.500
.000	0.02073	1.916	0.02171	1.583	0.02878	1.500
.000	0.02114	1.916	0.02217	1.583	0.02825	1.500
.916	0.02601	1.583	0.02912	1.500	0.02971	
.916	0.00696	1.583	0.00766	1.500	0.00784	
.916	0.00834	1.583	0.00908	1.500	0.00826	
.916	0.00855	1.583	0.00934	1.500	0.00952	
.916	0.00946	1.583	0.01036	1.500	0.01060	
.916	0.01024	1.583	0.01128	1.500	0.01152	
.916	0.01171	1.583	0.01287	1.500	0.01317	
.916	0.01491	1.583	0.01653	1.500	0.01689	
.916	0.01839	1.583	0.02143	1.500	0.02220	
.916	0.01091	1.583	0.01213	1.500	0.01244	
.916	0.00922	1.583	0.01006	1.500	0.01024	
.916	0.00885	1.583	0.00964	1.500	0.00982	
.916	0.02018	1.583	0.02383	1.500	0.02462	
.916	0.00793	1.583	0.00854	1.500	0.00872	
.916	0.00804	1.583	0.00865	1.500	0.00878	
.583	0.02436	1.500	0.02497			
.000	0.02528	1.916	0.02613	1.666	0.02859	1.500
.000	0.01570	1.916	0.01618	1.666	0.01745	1.500
.000	0.01030	1.916	0.01055	1.666	0.01140	1.500
.916	0.00728	1.666	0.00781	1.500	0.00817	
.000	0.00718	1.916	0.00736	1.666	0.00798	1.500
.000	0.00987	1.916	0.01042	1.666	0.01171	1.500
.000	0.01816	1.916	0.01933	1.666	0.02301	1.500
.000	0.03969	1.916	0.04190	1.666	0.04485	1.500
.000	0.03380	1.916	0.03491	1.666	0.03767	1.500
.000	0.03301	1.916	0.03416	1.666	0.03723	1.500
.000	0.12946	1.916				
.000	0.02598	1.916	0.02695	1.666	0.02970	1.500
.000	0.04458	1.916	0.04571	1.666	0.04988	1.500
.000	0.01124	1.916	0.01471	1.666	0.01622	1.500
.000	0.01317	1.916	0.01371	1.666	0.01512	1.500
.000	0.01383	1.916	0.01455	1.666	0.01671	1.500
.000	0.01012	1.916	0.01080	1.666	0.01264	1.500
.000	0.01407	1.916	0.01491	1.666	0.01706	1.500
.000	0.01917	1.916	0.02042	1.666	0.02417	1.500
.000	0.01687	1.916	0.01766	1.666	0.01963	1.500
.000	0.01675	1.916	0.01757	1.666	0.01970	1.500
.000	0.03108	1.916	0.03479	1.666	0.04527	
.000	0.01982	1.916	0.02041	1.666	0.02207	1.500
.000	0.01642	1.916	0.01699	1.666	0.01855	1.500
.000	0.01752	1.916	0.01842	1.666	0.02048	1.500
.000	0.01779	1.916	0.01859	1.666	0.02055	1.500
.000	0.02359	1.916	0.02487	1.666	0.02814	1.500
.000	0.02095	1.916	0.02327	1.666	0.02827	1.500

d Air

Time Sec After Spark	Probe Ft From Center	Time Sec After Spark	Probe Ft From Center	Time Sec After Spark
0.02185	1.583	0.02585	1.500	0.02701
0.02175	1.583	0.02693	1.500	0.02765
0.02067	1.583	0.02537	1.500	0.02610
0.02171	1.583	0.02878	1.500	0.02927
0.02217	1.583	0.02825	1.500	0.02934
0.02912	1.500	0.02971		
0.00766	1.500	0.00784		
0.00908	1.500	0.00826		
0.00934	1.500	0.00952		
0.01036	1.500	0.01060		
0.01128	1.500	0.01152		
0.01287	1.500	0.01317		
0.01653	1.500	0.01689		
0.02143	1.500	0.02220		
0.01213	1.500	0.01244		
0.01006	1.500	0.01024		
0.00964	1.500	0.00982		
0.02383	1.500	0.02462		
0.00854	1.500	0.00872		
0.00865	1.500	0.00878		
0.02497				
0.02613	1.666	0.02859	1.500	0.03018
0.01618	1.666	0.01745	1.500	0.01818
0.01055	1.666	0.01140	1.500	0.01195
0.00781	1.500	0.00817		
0.00736	1.666	0.00798	1.500	0.00840
0.01042	1.666	0.01171	1.500	0.01257
0.01933	1.666	0.02301	1.500	0.02472
0.04190	1.666	0.04485	1.500	0.06086
0.03491	1.666	0.03767	1.500	0.03896
0.03416	1.666	0.03723	1.500	0.03880
0.02695	1.666	0.02970	1.500	0.03122
0.04571	1.666	0.04988	1.500	0.06851
0.01471	1.666	0.01622	1.500	0.01703
0.01371	1.666	0.01512	1.500	0.01591
0.01455	1.666	0.01671	1.500	0.01766
0.01080	1.666	0.01264	1.500	0.01350
0.01491	1.666	0.01706	1.500	0.01838
0.02042	1.666	0.02417	1.500	0.02601
0.01766	1.666	0.01963	1.500	0.02098
0.01757	1.666	0.01970	1.500	0.02083
0.03479	1.666	0.04527		
0.02041	1.666	0.02207	1.500	0.02302
0.01699	1.666	0.01855	1.500	0.01942
0.01842	1.666	0.02048	1.500	0.02152
0.01859	1.666	0.02055	1.500	0.02153
0.02487	1.666	0.02814	1.500	0.02964
0.02327	1.666	0.02827	1.500	0.03137

Table A-2. Centrifuge Test

Run	Probe Ft From Center	Time Sec After Spark	Probe Ft From Center	Time Sec After Spark	Probe Ft From Center	Sec Af
101	2.416	0.01726	2.250	0.01940	2.000	0.
102	2.416	0.01445	2.25[illegible]	0.01642	2.000	0.
103	2.250	0.01045	2.000	0.01190	1.916	0.
104	2.250	0.01560	2.000	0.01815	1.916	0.
105	2.250	0.01494	2.000	0.01768	1.916	0.
106	2.250	0.01283	2.000	0.01446	1.916	0.
107	2.250	0.00928	2.166	0.01000	1.666	0.
108	2.416	0.00744	2.250	0.00835	2.000	0.
109	2.416	0.00936	2.250	0.01064	2.000	0.
110	2.416	0.00645	2.250	0.00733	2.000	0.
111	2.416	0.01257	2.250	0.01433	2.000	0.
112	2.416	0.00994	2.250	0.01195	2.000	0.
113	2.416	0.00878	2.250	0.01071	2.000	0.
114	2.416	0.01620	2.250	0.01834	2.000	0.
115	2.416	0.00825	2.250	0.01024	2.000	0.
116	2.416	0.01329	2.250	0.01537	2.000	0.
117	2.416	0.01134	2.250	0.01311	2.000	0.
118	2.416	0.00829	2.250	0.01012	2.000	0.
119	2.416	0.00729	2.250	0.00928	1.916	0.
120	2.416	0.00726	2.250	0.00939	2.000	0.
121	2.416	0.00707	2.250	0.00909	1.666	0.
122	2.416	0.00866	2.250	0.01146	2.000	0.
123	2.416	0.01418	2.250	0.01636	2.000	0.
124	2.416	0.01834	2.250	0.02123	2.000	0.
125	2.250	0.01585	2.000	0.01805	1.916	0.
126	2.250	0.00933	2.000	0.01218	1.666	0.
127	2.250	0.01207	2.000	0.01549	1.583	0.
128	2.416	0.00831	2.250	0.01028	2.000	0.
129	2.416	0.01935	2.250	0.02207	2.000	0.
130	2.416	0.00747	2.250	0.00932	2.000	0.
131	2.333	0.02085	2.250	0.02220	2.083	0.
132	2.333	0.00988	2.250	0.01176	2.083	0.
133	2.333	0.01006	2.250	0.01140	2.083	0.
134	2.333	0.04560	2.250	0.04765	2.083	0.
135	2.333	0.00915	2.083	0.01230	1.833	0.
136	2.333	0.00825	2.250	0.00922	2.083	0.
137	2.333	0.00821	2.250	0.00911	2.083	0.
138	2.333	0.00855	2.250	0.00936	2.083	0.
139	2.250	0.00910	2.083	0.01006	1.833	0.
140	2.250	0.00846	2.083	0.00931	1.833	0.
141	2.083	0.00938	1.666	0.01084	1.583	0.
142	2.250	0.00841	2.083	0.00935	1.666	0.
143	2.250	0.00785	2.083	0.00853	1.666	0.
144	2.250	0.00828	2.083	0.00911	1.833	0.
145	2.250	0.00805	2.083	0.00858	1.833	0.
146	2.250	0.03059	2.083	0.03391	1.833	0.
147	2.250	0.01373	2.083	0.01596	1.833	0.
157	2.250	0.05018	2.083	0.05710	1.833	0.
163	2.083	0.02091	1.833	0.02491	1.666	0.

Table A-2. Centrifuge Test Data for Propane and Air (Continued)

Probe Ft From Center	Time Sec After Spark	Probe Ft From Center	Time Sec After Spark	Probe Ft From Center	Time Sec After Spark	Ft F
2.000	0.02274	1.916	0.02405	1.666	0.02881	
2.000	0.01896	1.916	0.02017	1.666	0.02364	
1.916	0.01230	1.666	0.01333	1.500	0.01397	
1.916	0.01923	1.666	0.02363	1.583	0.02524	
1.916	0.01890	1.666	0.02341	1.583	0.02457	
1.916	0.01494	1.666	0.01620	1.583	0.01663	
1.666	0.01151	1.583	0.01175			
2.000	0.00927	1.916	0.00951	1.666	0.01018	
2.000	0.01187	1.916	0.01228	1.666	0.01327	
2.000	0.00826	1.916	0.00855	1.666	0.00913	
2.000	0.01608	1.916	0.01661	1.666	0.01801	
2.000	0.01385	1.916	0.01444	1.666	0.01586	
2.000	0.01296	1.916	0.01357	1.666	0.01520	
2.000	0.02110	1.916	0.02227	1.666	0.02669	
2.000	0.01217	1.916	0.01277	1.666	0.01410	
2.000	0.01866	1.916	0.02043	1.666	0.02598	
2.000	0.01500	1.916	0.01555	1.666	0.01701	
2.000	0.01244	1.916	0.01317	1.666	0.01488	
1.916	0.01253	1.666	0.01434	1.500	0.01530	
2.000	0.01195	1.666	0.01463	1.500	0.01573	
1.666	0.01482					
2.000	0.01482	1.666	0.01756			
2.000	0.01933	1.916	0.02061	1.666	0.02545	
2.000	0.02509	1.916	0.02650	1.666	0.03092	
1.916	0.01872	1.666	0.02049	1.583	0.02104	
1.666	0.01521	1.583	0.01582			
1.583	0.01848					
2.000	0.01298	1.583	0.01579			
2.000	0.02669	1.916	0.02882	1.666	0.03456	
2.000	0.01179	1.583	0.01426			
2.083	0.02451	1.916	0.02744	1.666	0.03220	
2.083	0.01406	1.833	0.01659	1.666	0.01776	
2.083	0.01297	1.833	0.01506	1.666	0.01610	
2.083	0.05133	1.833	0.05572	1.666	0.05910	
1.833	0.01442	1.666	0.01564	1.583	0.01612	
2.083	0.01096	1.833	0.01295	1.666	0.01404	
2.083	0.01042	1.833	0.01179	1.666	0.01238	
2.083	0.01006	1.833	0.01122	1.666	0.01203	
1.833	0.01127	1.666	0.01187	1.583	0.01223	
1.833	0.01034	1.666	0.01091	1.583	0.01114	
1.583	0.01107					
1.666	0.01082	1.583	0.01106			
1.666	0.01000	1.583	0.01025			
1.833	0.01041	1.666	0.01112	1.583	0.01136	
1.833	0.00923	1.666	0.00953	1.583	0.00964	
1.833	0.03929	1.583	0.04538	1.500	0.04728	
1.833	0.01753	1.583	0.01867	1.500	0.01910	
1.833	0.06562	1.666	0.07438	1.583	0.07911	
1.666	0.02754	1.583	0.02874			

(Continued)

Time Sec After Spark	Probe Ft From Center	Time Sec After Spark	Probe Ft From Center	Time Sec After Spark
0.02405	1.666	0.02881	..500	0.03167
0.02017	1.666	0.02364	1.500	0.02607
0.01323	1.500	0.01397		
0.02363	1.583	0.02524		
0.02341	1.583	0.02457		
0.01620	1.583	0.01663		
0.01175				
0.00951	1.666	0.01018	1.500	0.01055
0.01228	1.666	0.01327	1.500	0.01386
0.00855	1.666	0.00913	1.500	0.00953
0.01661	1.666	0.01801	1.500	0.01889
0.01444	1.666	0.01586	1.500	0.01675
0.01357	1.666	0.01520	1.500	0.01602
0.02227	1.666	0.02669	1.500	0.02939
0.01277	1.666	0.01410	1.500	0.01494
0.02043	1.666	0.02598	1.500	0.02835
0.01555	1.666	0.01701	1.500	0.01793
0.01317	1.666	0.01488	1.500	0.01591
0.01434	1.500	0.01530		
0.01463	1.500	0.01573		
0.01756				
0.02061	1.666	0.02545		
0.02650	1.666	0.03092		
0.02049	1.583	0.02104		
0.01582				
0.01579				
0.02882	1.666	0.03456		
0.01426				
0.02744	1.666	0.03220		
0.01659	1.666	0.01776	1.583	0.01829
0.01506	1.666	0.01610	1.583	0.01680
0.05572	1.666	0.05910		
0.01564	1.583	0.01612		
0.01295	1.666	0.01404	1.583	0.01446
0.01179	1.666	0.01238	1.583	0.01268
0.01122	..666	0.01203	1.583	0.01227
0.01187	1.583	0.01223		
0.01091	1.583	0.01114		
0.01106				
0.01025				
0.01112	1.583	0.01136		
0.00953	1.583	0.00964		
0.04538	1.500	0.04728		
0.01867	1.500	0.01910		
0.07438	1.583	0.07911		
0.02874				

Table A-2. Centrifuge Test Data

Run	Probe Ft From Center	Time Sec After Spark	Probe Ft From Center	Time Sec After Spark	Probe Ft From Center	Ti Sec Afte
252	2.250	0.1356	2.083	0.1270	1.833	0.10
258	2.250	0.2421	2.083	0.2226	1.833	0.15
259	2.083	0.2319	1.833	0.1361	1.666	0.10
265	2.250	0.2437	2.083	0.2340	1.833	0.15
266	2.250	0.1275	2.083	0.1203	1.833	0.10
267	2.250	0.0709	2.083	0.0636	1.833	0.05
270	2.250	0.1155	2.083	0.0971	1.833	0.07
272	2.250	0.1139	2.083	0.1053	1.833	0.09
273	2.250	0.1550	2.083	0.1407	1.833	0.10
274	2.250	0.1688	2.083	0.1522	1.833	0.12
275	1.833	0.1293	1.666	0.1058	1.583	0.09
276	2.250	0.1927	2.083	0.1799	1.833	0.15
277	2.250	0.2248	2.083	0.2049	1.833	0.16
278	1.833	0.1710	1.666	0.1097	1.583	0.08
279	2.250	0.2447	2.083	0.2096	1.833	0.13
280	2.250	0.2195	2.083	0.2093	1.833	0.18
283	2.083	0.2757	1.833	0.2296	1.666	0.20
285	2.250	0.0951	2.083	0.0907	1.833	0.07
287	2.250	0.1340	2.083	0.1257	1.833	0.09
288	2.250	0.1609	2.083	0.1560	1.833	0.12
289	2.250	0.1850	2.083	0.1792	1.833	0.14
290	2.250	0.1786	2.083	0.1728	1.833	0.15
291	2.250	0.1942	2.083	0.1883	1.833	0.17
292	2.250	0.2053	2.083	0.2000	1.833	0.17
295	2.250	0.2396	2.083	0.2333	1.833	0.22
296	2.250	0.2583	2.083	0.2490	1.833	0.23
298	2.250	0.1903	2.083	0.1850	1.833	0.16
305	2.083	0.2434	1.833	0.2078	1.666	0.16
306	2.083	0.1874	1.833	0.1587	1.666	0.12
307	2.083	0.2176	1.833	0.1878	1.666	0.16
309	2.083	0.2255	1.833	0.1966	1.666	0.17
310	2.083	0.2616	1.833	0.2217	1.666	0.20
315	2.083	0.2328	1.833	0.1971	1.666	0.12
316	2.083	0.2683	1.833	0.2000	1.666	0.15
317	2.083	0.2623	1.833	0.2034	1.666	0.16
319	2.083	0.3024	1.833	0.2327	1.666	0.19
324	1.666	0.1754	1.583	0.1556		
326	1.666	0.2245	1.583	0.1769		
329	2.083	0.1995	1.833	0.1652	1.666	0.13
336	1.833	0.2049	1.666	0.1451	1.583	0.11
338	1.666	0.1296	1.583	0.1087		
362	2.083	0.1351	1.833	0.1139	1.666	0.09
363	2.083	0.2401	1.833	0.2043	1.666	0.16
364	2.083	0.2153	1.833	0.1756	1.666	0.14
374	2.083	0.0748	1.833	0.0592	1.666	0.05
376	2.083	0.1700	1.833	0.1461	1.666	0.12
377	2.083	0.1198	1.833	0.0981	1.666	0.08
382	2.083	0.2757	1.833	0.2583	1.666	0.24
384	2.083	0.3816	1.833	0.3701	1.666	0.34

Table A-2. Centrifuge Test Data for Propane and Air (Continued)

me Spark	Probe Ft From Center	Time Sec After Spark	Probe Ft From Center	Time Sec After Spark	Probe Ft From Center	Time Sec After Spar
0	1.833	0.1006	1.666	0.0785	1.583	0.0670
5	1.833	0.1502	1.666	0.1432	1.583	0.1266
1	1.666	0.1031	1.583	0.0772		
0	1.833	0.1505	1.666	0.1053	1.583	0.0816
8	1.833	0.1029	1.666	0.0899	1.583	0.0807
5	1.833	0.0578	1.666	0.0519	1.583	0.0490
1	1.833	0.0782	1.666	0.0631	1.583	0.0529
8	1.833	0.0942	1.666	0.0837	1.583	0.0783
7	1.833	0.1014	1.666	0.0856	1.583	0.0794
2	1.833	0.1229	1.666	0.1039	1.583	0.0990
8	1.583	0.0942				
0	1.833	0.1500	1.666	0.1284	1.583	0.1211
8	1.833	0.1694	1.666	0.1354	1.583	0.1170
1	1.583	0.0855				
8	1.833	0.1317	1.666	0.0779	1.583	0.0596
8	1.833	0.1849	1.666	0.1449	1.583	0.1210
1	1.666	0.2083	1.583	0.1791		
8	1.833	0.0795	1.666	0.0698	1.583	0.0654
8	1.833	0.0956	1.666	0.0791	1.583	0.0675
8	1.833	0.1295	1.666	0.0874	1.583	0.0720
8	1.833	0.1464	1.666	0.0899	1.583	0.0739
8	1.833	0.1510	1.666	0.0918	1.583	0.0748
8	1.833	0.1723	1.666	0.1107	1.583	0.0830
8	1.833	0.1714	1.666	0.1015	1.583	0.0689
8	1.833	0.2227	1.666	0.1908	1.583	0.1517
8	1.833	0.2384	1.666	0.2364	1.583	0.1631
8	1.833	0.1633	1.666	0.1203	1.583	0.0879
1	1.666	0.1634	1.583	0.1449		
1	1.666	0.1238	1.583	0.1131		
1	1.666	0.1634	1.583	0.1371		
1	1.666	0.1701	1.583	0.1510		
1	1.666	0.2035	1.583	0.1847		
1	1.666	0.1289	1.583	0.1088		
1	1.666	0.1591	1.583	0.1356		
1	1.666	0.1696	1.583	0.1483		
1	1.666	0.1914	1.583	0.1577		
	1.666	0.1333	1.583	0.1142		
	1.583	0.1162				
	1.666	0.0990	1.583	0.0851		
	1.666	0.1609	1.583	0.1512		
	1.666	0.1488	1.583	0.1287		
	1.666	0.0505	1.583	0.0466		
	1.666	0.1218	1.583	0.1078		
	1.666	0.0845	1.583	0.0768		
	1.666	0.2466	1.583	0.2228		
	1.666	0.3536	1.583	0.3416		

d Air (Continued)

Probe From Center	Time Sec After Spark	Probe Ft From Center	Time Sec After Spark	Probe Ft From Center	Time Sec After Spark
1.666	0.0785	1.583	0.0670		
1.666	0.1432	1.583	0.1266		
1.583	0.0772				
1.666	0.1053	1.583	0.0816		
1.666	0.0899	1.583	0.0807		
1.666	0.0519	1.583	0.0490		
1.666	0.0631	1.583	0.0529		
1.666	0.0837	1.583	0.0783		
1.666	0.0856	1.583	0.0794		
1.666	0.1039	1.583	0.0990		
1.666	0.1284	1.583	0.1211		
1.666	0.1354	1.583	0.1170		
1.666	0.0779	1.583	0.0596		
1.666	0.1119	1.583	0.1210		
1.583	0.1791				
1.666	0.0698	1.583	0.0654		
1.666	0.0791	1.583	0.0675		
1.666	0.0874	1.583	0.0720		
1.666	0.0899	1.583	0.0739		
1.666	0.0918	1.583	0.0748		
1.666	0.1107	1.583	0.0830		
1.666	0.1015	1.583	0.0689		
1.666	0.1908	1.583	0.1517		
1.666	0.2364	1.583	0.1631		
1.666	0.1203	1.583	0.0879		
1.583	0.1119				
1.583	0.1131				
1.583	0.1371				
1.583	0.1510				
1.583	0.1847				
1.583	0.1088				
1.583	0.1356				
1.583	0.1483				
1.583	0.1577				
1.583	0.1142				
1.583	0.0851				
1.583	0.1512				
1.583	0.1287				
1.583	0.0466				
1.583	0.1078				
1.583	0.0768				
1.583	0.2228				
1.583	0.3416				

Table A-2. Centrifuge Test Data fo

Run	Probe Ft From Center	Time Sec After Spark	Probe Ft From Center	Time Sec After Spark	Probe Ft From Center	Ti Sec Afte
387	2.083	0.5268	1.833	0.5072	1.666	0.4
389	2.083	0.2726	1.833	0.1678	1.666	0.1
390	2.083	0.0815	1.833	0.0629	1.666	0.0
391	2.083	0.1585	1.833	0.1268	1.666	0.1
392	2.083	0.2178	1.833	0.1966	1.666	0.1
395	2.083	0.2362	1.833	0.2193	1.666	0.1
399	2.083	0.3818	1.833	0.3636	1.666	0.3
400	2.083	0.3101	1.833	0.2859	1.666	0.2
101	2.083	0.3302	1.833	0.3142	1.666	0.2
403	2.083	0.2353	1.833	0.2092	1.666	0.1
404	2.083	0.2263	1.833	0.1985	1.666	0.1
405	2.083	0.2254	1.833	0.2124	1.666	0.2
406	2.083	0.2039	1.833	0.1859	1.666	0.1
407	2.083	0.2185	1.833	0.1924	1.666	0.1
408	2.083	0.2889	1.833	0.2705	1.666	0.2

entrifuge Test Data for Propane and Air (Continued)

Probe om Center	Time Sec After Spark	Probe Ft From Center	Time Sec After Spark	Probe Ft From Center	Time Sec After Spark	Probe Ft From C
.666	0.4938	1.583	0.4833			
.666	0.1351	1.583	0.1269			
.666	0.0542	1.583	0.0483			
.666	0.1029	1.583	0.0897			
.666	0.1351	1.583	0.1115			
.666	0.1778	1.583	0.1246			
.666	0.3320	1.583	0.3053			
.666	0.2749	1.583	0.2749			
.666	0.2810	1.583	0.2629			
.666	0.1947	1.583	0.1918			
.666	0.1893	1.583	0.1785			
.666	0.2053	1.583	0.1919			
.666	0.1651	1.583	0.1587			
.666	0.1673	1.583	0.1493			
.666	0.2415	1.583	0.2299			

nd Air (Continued)

Probe Ft From Center	Time Sec After Spark	Probe Ft From Center	Time Sec After Spark	Probe Ft From Center	Time Sec After Spark
1.583	0.4833				
1.583	0.1269				
1.583	0.0483				
1.583	0.0897				
1.583	0.1115				
1.583	0.1246				
1.583	0.3053				
1.583	0.2749				
1.583	0.2629				
1.583	0.1918				
1.583	0.1785				
1.583	0.1919				
1.583	0.1587				
1.583	0.1493				
1.583	0.2299				

Table A-3. Centrifuge Test Conditions for Hydrogen and Air

Run	f/a	Pressure, psia	Temperature, °F	Pipe Size
220	0.029	5	105	0
221	0.029	5	105	50
222	0.029	5	110	100
223	0.029	5	106	150
224	0.029	5	110	200
225	0.029	5	103	300
226	0.029	5	110	600
227	0.029	5	105	1,200
228	0.029	5	112	2,112
229	0.029	5	108	2,110
234	0.013	5	Unrecorded	0
235	0.013	5	98	750
236	0.013	5	96	1,000
240	0.013	15	106	0
241	0.013	15	106	1,500
243	0.013	10	105	0
245	0.013	10	110	1,500
247	0.013	10	110	1,750
248	0.013	10	100	1,750

Table A-4. Centrifuge Test Data f

Run	Probe Ft From Center	Time Sec After Spark	Probe Ft From Center	Time Sec After Spark	Probe Ft From Center
220	2.250	0.01875	2.083	0.01635	1.833
221	2.250	0.01962	2.083	0.01722	1.833
222	2.250	0.01947	2.083	0.01731	1.833
223	2.250	0.01744	2.083	0.01549	1.833
224	2.250	0.01963	2.083	0.01720	1.833
225	2.250	0.01768	2.083	0.01561	1.833
226	2.250	0.01744	2.083	0.01561	1.833
227	2.250	0.02305	2.083	0.02110	1.833
228	2.250	0.04671	2.083	0.04500	1.833
229	2.250		2.083		1.833
234	2.250	0.1355	2.083	0.1254	1.833
235	2.250	0.1109	2.083	0.0989	1.833
236	2.250	0.1721	2.083	0.1612	1.666
240	2.250	0.0867	2.083	0.0801	1.833
241	2.250	0.0795	2.083	0.0746	1.833
243	2.250	0.1026	2.083	0.0911	1.833
245	2.250	0.0998	2.083	0.0954	1.833
246	2.250	0.0998	2.083	0.0960	1.833
248	2.250	0.1056	2.083	0.1016	1.833

trifuge Test Data for Hydrogen and Air

Probe Ft From Center	Time Sec After Spark	Probe Ft From Center	Time Sec After Spark	Probe Ft From Center	Time Sec After Spark
1.833	0.01442	1.666	0.01154	1.583	0.01106
1.833	0.01438	1.666	0.01196	1.583	0.01148
1.833	0.01490	1.666	0.01226	1.583	0.01202
1.833	0.01476	1.666	0.01195	1.583	0.01171
1.833	0.01488	1.666	0.01195	1.583	0.01146
1.833	0.01476	1.666	0.01195	1.583	0.01171
1.833	0.01451	1.666	0.01207	1.583	0.01146
1.833	0.01780	1.666	0.01549	1.583	0.01500
1.833	0.04146	1.666	0.03549	1.583	0.03037
1.833		1.666		1.583	
1.833	0.1202	1.666	0.0913	1.583	0.0860
1.833	0.0812	1.666	0.0724	1.583	0.0676
1.666	0.1331	1.583	0.1243		
1.833	0.0693	1.666	0.0626	1.583	0.0601
1.833	0.0693	1.583	0.0626		
1.833	0.0760	1.666	0.0672	1.583	0.0617
1.833	0.0915	1.666	0.0838	1.583	0.0798
1.833	0.0851	1.583	0.0759		
1.833	0.0919	1.583	0.0789		

Table A-5. PVC Pipe Test Conditions

Run	f/a	Pressure, psia	Temperature	Pipe Size, in.	Fuel
1 P	0.064	5.0	Ambient	2	Propane
2 P	0.064	14.0	Ambient	2	Propane
3 P	0.064	14.7	Ambient	2	Propane
4 P	0.064	14.0	Ambient	2	Propane
5 P	0.064	14.7	Ambient	2	Propane
6 P	0.064	14.7	Ambient	2	Propane
7 P	0.064	10.0	Ambient	2	Propane
8 P	0.064	10.0	Ambient	2	Propane
9 P	0.064	10.0	Ambient	2	Propane
10 P	0.064	10.0	Ambient	4	Propane
11 P	0.064	5.0	Ambient	4	Propane
12 P	0.064	14.7	Ambient	4	Propane
13 P	0.064	10.0	Ambient	4	Propane
14 P	0.064	10.0	Ambient	4	Propane
15 P	0.064	14.0	Ambient	4	Propane
17 P	0.064	10.0	Ambient	6	Propane
18 P	0.064	14.7	Ambient	6	Propane
19 P	0.064	14.0	Ambient	6	Propane
20 P	0.064	5.0	Ambient	6	Propane
21 P	0.064	14.0	Ambient	6	Propane
22 P	0.029	14.7	Ambient	6	Hydrogen
23 P	0.029	14.7	Ambient	6	Hydrogen
24 P	0.029	14.7	Ambient	4	Hydrogen
25 P	0.029	14.7	Ambient	2	Hydrogen
26 P	0.029	14.7	Ambient	2	Hydrogen
27 P	0.029	5.0	Ambient	2	Hydrogen

Ta

Run	Probe 1 In. From Center	Time Sec After Spark	Probe 2 In. From Center	Time Sec After Spark	Probe 2 In. From Center	Sec
1 P	0.0	0.03679	0.70	0.05873	0.35	
2 P	0.0	0.01865	0.70	0.02455	0.35	
3 P	0.0	0.01847	0.70	0.02369	0.35	
4 P	0.0	0.01819	0.70	0.02223	0.35	
5 P	0.0	0.01386	0.70	0.01795	0.35	
6 P	0.0	0.01418	0.70	0.01848	0.35	
7 P	0.0	0.02133	0.70	0.03458	0.35	
8 P	0.0	0.02145	0.70	0.03337	0.35	
9 P	0.0	0.02110	0.70	0.03512	0.35	
10 P	0.0	0.03195	1.60	0.04500	0.80	
11 P	0.0	0.02976	1.60	0.08366	0.80	
12 P	0.0	0.02451	1.60	0.03146	0.80	
13 P	0.0	0.02953	1.60	0.04419	0.80	
14 P	0.0	0.03085	1.60	0.04329	0.80	
15 P	0.0	0.02585	1.60	0.03220	0.80	
17 P	0.0	0.03866	2.66	0.04500	1.33	
18 P	0.0	0.03110	2.66	0.03805	1.33	
19 P	0.0	0.02695	2.66	0.04549	1.33	
20 P	0.0	0.05744	2.66	0.11134	1.33	
21 P	0.0	0.02707	2.66	0.06305	1.33	
22 P	0.0	0.01024	2.66	0.01159	1.33	
23 P	0.0	0.01200	2.66	0.01679	1.33	
24 P	0.0	0.00578	1.60	0.00741	0.80	
25 P	0.0	0.00378	0.70	0.00518	0.35	
26 P	0.0	0.00372	0.70	0.00512	0.35	
27 P	0.0	0.00646	0.70	0.01354	0.35	

NOTE:

Probe 1 - Located 1 ft axially from spark plug.
Probe 2 - Located 2 ft axially from spark plug.

Table A-6. PVC Pipe Data

Probe 2 In. From Center	Time Sec After Spark	Probe 2 In. From Center	Time Sec After Spark	Probe 2 In. From Center	Time Sec After Spark
0.35	0.05867	0.0	0.05861	-0.35	0.05867
0.35	0.02444	0.0	0.02438	-0.35	0.02438
0.35	0.02358	0.0	0.02347	-0.35	0.02330
0.35	0.02211	0.0	0.02211	-0.35	0.02217
0.35	0.01780	0.0	0.01773	-0.35	0.01773
0.35	0.01830	0.0	0.01824	-0.35	0.01830
0.35	0.03434	0.0	0.03422	-0.35	0.03422
0.35	0.03277	0.0	0.03265	-0.35	0.03277
0.35	0.03488	0.0	0.03463	-0.35	0.03488
0.80	0.04500	0.0		-0.80	0.04463
0.80	0.08427	0.0	0.08439	-0.80	0.08378
0.80	0.03061	0.0	0.03049	-0.80	0.03061
0.80	0.04442	0.0	0.04442	-0.80	0.04442
0.80	0.04280	0.0	0.04268	-0.80	0.04293
0.80	0.03146	0.0	0.03134	-0.80	0.03146
1.33	0.04305	0.0		-1.33	0.04305
1.33	0.03671	0.0		-1.33	0.03659
1.33	0.04195	0.0		-1.33	0.04171
1.33	0.11085	0.0	0.11134	-1.33	0.11134
1.33	0.05878	0.0	0.05829	-1.33	0.05732
1.33	0.01146	0.0		-1.33	0.01146
1.33	0.01661	0.0		-1.33	0.01673
0.80	0.00729	0.0	0.00717	-0.80	0.00729
0.35	0.00518	0.0	0.00518	-0.35	0.00518
0.35	0.00506	0.0		-0.35	0.00512
0.35	0.01354	0.0		-0.35	0.01354

nter	Time Sec After Spark	Probe 2 In. From Center	Time Sec After Spark	Probe 2 In. From Center	Time Sec After Spark
	0.05861	-0.35	0.05867	-0.70	0.05879
	0.02438	-0.35	0.02438	-0.70	0.02449
	0.02347	-0.35	0.02330	-0.70	0.02341
	0.02211	-0.35	0.02217	-0.70	0.02247
	0.01773	-0.35	0.01773	-0.70	0.01803
	0.01824	-0.35	0.01830	-0.70	0.01836
	0.03422	-0.35	0.03422	-0.70	0.03446
	0.03265	-0.35	0.03277	-0.70	0.03325
	0.03463	-0.35	0.03488	-0.70	0.03549
		-0.80	0.04463	-1.60	0.04463
	0.08439	-0.80	0.08378	-1.60	0.08402
	0.03049	-0.80	0.03061	-1.60	0.03098
	0.04442	-0.80	0.04442	-1.60	0.04419
	0.04268	-0.80	0.04293	-1.60	0.04268
	0.03134	-0.80	0.03146	-1.60	0.03171
		-1.33	0.04305	-2.66	0.04293
		-1.33	0.03659	-2.66	0.03634
		-1.33	0.04171	-2.66	0.04134
	0.11134	-1.33	0.11134	-2.66	0.11110
	0.05829	-1.33	0.05732	-2.66	0.05744
		-1.33	0.01146	-2.66	0.01134
		-1.33	0.01673	-2.66	0.01703
	0.00717	-0.80	0.00729	-1.60	0.00747
	0.00518	-0.35	0.00518	-0.70	0.00518
		-0.35	0.00512	-0.70	0.00512
		-0.35	0.01354	-0.70	0.01354

APPENDIX B
CENTRIFUGE COMBUSTION PROCESS

The combustion process in a closed, rotating pipe is very complex to model. The model must include flame bubble mechanics, pressure rise due to burning, hot gas expansion, and constantly changing parameters of the burned and unburned gases. The present analysis was limited to the initial portion of burning and, therefore, certain simplifying assumptions were made. These were:

1. The temperature of the burned gas was constant
2. The velocity of the burned gas was zero.

After ignition, the flamefront travels down the tube at an observed velocity, S_o. The cold, unburned gas travels at S_a, caused by the thermal expansion of the hot gas. If one is riding the flamefront, the cold gas is entering at the bubble velocity, S_B, and leaving at the observed velocity, S_o. From the conservation of mass, neglecting unsteady terms, we get:

$$\rho_a S_B \qquad \rho_B S_o \qquad \text{Eq (22)}$$

where

ρ_a cold gas density

S_B true flame velocity

ρ_B = hot, burned gas density

S_o = observed flamespeed.

Neglecting unsteady terms proved to be a valid assumption in this case because density changes were relatively small.

The basic bubble equation can be written as

$$\frac{d^2R}{dt^2} \cdot -\frac{\rho_a}{\rho_B}\left(1 - \frac{\rho_B}{\rho_a}\right) R\omega^2 \cdot \frac{\rho_a}{\rho_B}\left(\frac{A_B C_D}{2 V_B}\right)\left(\frac{dR}{dt}\right)^2 \qquad \text{Eq (23)}$$

where all terms have been defined previously. If a value for $A_B C_D/2\ V_B$ is assumed, the differential equation can be solved numerically if ρ_B and ρ_a are calculated as functions of time. Initially, we can state:

$$\frac{\rho_B}{\rho_a} = \frac{P_B/\tilde{R}_B T_B}{P_a/\tilde{R}_a T_a} \approx \frac{T_a}{T_B} \qquad \text{Eq (24)}$$

where

ρ = density

P = pressure

T = temperature

$\tilde{R}$ = gas constant

subscript B bubble

subscript a cold.

The change in density can be calculated from the mass fraction burned during each time iteration assuming constant pressure and burned gas temperature. A new pressure is calculated from the fraction of mass burned, and this process is repeated down the tube. A flow diagram is presented in figure B-1, followed by a listing of the computer program and a sample result.

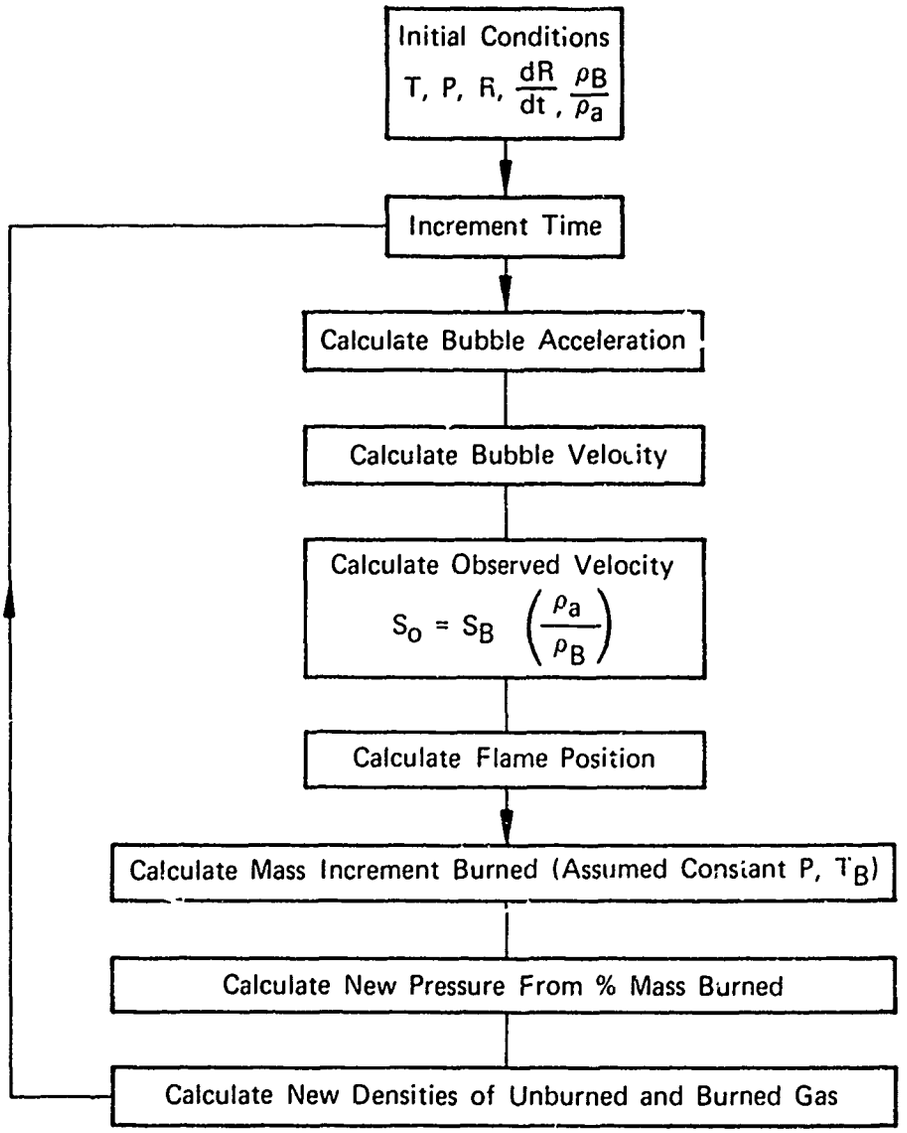

T = Temperature
P = Pressure
R = Flame Position
$\frac{dR}{dt}$ = Bubble Velocity
$\frac{\rho_B}{\rho_a}$ = Density Ratio

Figure B-1. Flow Diagram FD 89714

```
HO IMPL .V (1  RELEASE 2.0          MAIN          DATE = 75077      10/11/28          PAGE 0001

0001                REAL M1,M1
0002                R1DOT(R2,OMEGA,RHO,CDU2L,R,DUT)=-R2*OMEGA**2//RHO*(1.0-RHO)* CDU2L
                   1/RHO*R1DOT**2
0003                DELTAT = .00001
0004          10000 READ(5,10001,END=99999) P1,TADIA,TCV,RPM
0005          10001 FORMAT(4F10.0)
0006                TIN1 = 530.
0007                GASC = 1716.
0008                OMEGA = 3.1415*2.*RPM/30.
0009                P1 = P1*144.
0010                RHI = P1/GASC/TINT
0011                RHO = TIN1/TADIA
0012                R2 = 3.0
0013                T = 0.0
0014                AREA = 3.1417*(1.375/12.)**2
0015                M1 = AREA*0.60*P1/GASC/TINT
0016                PP = RHI*GASC*TCV
0017                M1 = 0.0
0018                CDU2L = 55.0
0019                R2DOT = 0.0
0020                R1DOT = 0.0
0021                P1 = P1
0022                R1DOT = R1DOT(R2,OMEGA,RHO,CDU2L,R1DOT)
0023                T1 = TIN1
0024                WRITE(6,8) P1,TADIA,TCV,RPM
0025             8 FORMAT(1H1,'****** P = ',F6.1,'    **** TADIA = ',F6.1,'    ****TCV =
                   1 ',F6.1,'     ****RPM = ',F6.2)
0026                WRITE(6,9)
0027             9 FORMAT('          TIME          R2          V2          V1
                   1  A1          RHO          P          TEMP')
0028                KOUNT = 0
0029            15 IF((KOUNT/10)*10 - KOUNT).EQ.0)
                   1WRITE(6,20)T,R2,R2DOT,R1DOT,R1DDOT,RHO,P1,T1
0030            20 FORMAT(F15.5)
0031               KOUNT = KOUNT+1
0032               IF(R2.LE.1.5) GO TO 10000
0033               T = T+DELTAT
0034               R1DOT = R1DOT+DELTAT + R1DOT
0035               R2DOT = R1DOT/RHO
0036               R2P = R2
0037               R2 = R2DOT*DELTAT + R2
0038               M1 = AREA*(R2P-R2)*P1/GASC/TADIA + M1
0039               RHI = (P1-M1)/AREA/(R2*3.0)
0040               P1 = M1/M1*(PP-P1) + P1
0041               T1 = P1/GASC/RP1
0042               RHO = M1/AREA/(3.0*R2)
0043               RHO = P1/RHI
0044               R1DDOT = R1DOT(R2,OMEGA,RHO,CDU2L,R1DOT)
0045               GO TO 10
0046          99999 STOP
0047                END
```

TIME			VI	AI	RHO	P	TEMP
0.0	0.0	0.0	0.0		0.12703	2161.00000	540.00000
0.00010					0.12718	2171.36965	540.62800
0.00020				174.00000	0.12748	2189.22778	541.69716
0.00030					0.12817	2207.44067	542.63419
0.00040					0.12885	2225.72106	543.45259
0.00050					0.12953	2244.05981	544.14180
0.00060					0.13021	2262.45284	544.70166
0.00070					0.12988	2280.89966	544.03174
0.00080					0.12956	2299.39869	543.93203
0.00090					0.12922	2317.94751	543.60278
0.00100					0.12889	2336.54492	543.34351
0.00110					0.12855	2355.18970	543.05347
0.00120					0.12821	2373.87915	542.73340
0.00130					0.12786	2392.61133	542.38281
0.00140					0.12752	2411.38452	542.00146
0.00150					0.12717	2430.19727	541.56960
0.00160					0.12681	2449.04712	541.14097
0.00170					0.12646	2467.93164	540.67358
0.00180					0.12610	2486.84912	540.16870
0.00190					0.12574	2505.79687	539.63306
0.00200					0.12538	2524.77246	539.06616
0.00210					0.12501	2543.77417	538.46851
0.00220					0.12464	2562.79858	537.83911
0.00230					0.12427	2581.84302	537.17896
0.00240					0.12390	2600.90625	536.48730
0.00250					0.12352	2619.98511	535.76440
0.00260					0.12314	2639.07617	535.01074
0.00270					0.12276	2658.17651	534.22534
0.00280					0.12238	2677.28394	533.40942
0.00290					0.12200	2696.39307	532.56226
0.00300					0.12161	2715.50244	531.68335
0.00310					0.12122	2734.60913	530.77368
0.00320					0.12083	2753.70972	529.83374
0.00330					0.12043	2772.80127	528.86304
0.00340					0.12004	2791.87842	527.86182
0.00350					0.11964	2810.94214	526.83057
0.00360					0.11924	2829.98560	525.76904
0.00370					0.11884	2849.00360	524.67798

APPENDIX C
SWIRL AUGMENTOR MODEL

The swirl augmentor model assumed a hot flame bubble was driven toward the center by centrifugal forces produced by the swirling flow and moved axially by the flow of air through the augmentor. The flame bubble location was calculated from the axial and radial movements of the bubble. The two movements were assumed to be independent. The axial movement of the flame bubble was calculated from the axial velocity of the cold unburned gases, which increased down the duct due to pressure losses. The radial movement of the flame bubble was more involved and will be discussed in detail. The model allowed a small fraction of combustible gases to burn, followed by an expansion of the burned gases. Another small fraction was burned, followed by another expansion. This process was repeated until all of the combustible mixture was burned.

For the burning step, the burning rate was calculated from equation 4. This required three terms to be calculated at each axial station: the rotational rate (ω), the density ratio (ρ_B/ρ_a), and $2V_B/A_E C_D$. Of these three terms, the rotational rate required the most analysis and will be discussed first.

To calculate ω, an analysis of the swirling flow was required. The flow immediately downstream of the vanes can be analyzed if the total enthalpy and the entropy are assumed radially constant and the radial equilibrium is approximated by

$$\frac{g}{\rho}\frac{dp}{dr} = \frac{V_u^2}{r} \qquad \text{Eq (25)}$$

where

- g = Gravitational acceleration
- ρ = Density
- p = Pressure
- V_u = Tangential velocity
- r = Radial position.

From Glassman (Reference 6), these assumptions result in the following equation downstream of the vanes

$$\frac{V_u^2}{r} + \frac{1}{2}\frac{d\left(V_u^2\right)}{dr} + \frac{1}{2}\frac{d\left(V_x^2\right)}{dr} = 0 \qquad \text{Eq (26)}$$

where V_x = axial velocity.

For the case of swirl vanes with radially constant turning angle a, equation 26 can be integrated to

$$\frac{V_u}{V_{u_c}} = \frac{V_x}{V_{x_c}} = \left(\frac{r}{r_c}\right)^{-\mathrm{Sin}^2 a} \qquad \text{Eq (27)}$$

where r_c represents the radius of half the total cross-sectional area and V_{u_c} and V_{x_c} represent the tangential and axial velocities at r_c. Figure C-1 shows V_u/V_{u_c} and V_x/V_{x_c} vs radius for swirl vanes of 35 degrees. For the case of small vane angles ($\leq$ 35 degrees), the flow can be approximated by radially constant tangential and axial velocities. Thus, the angular rotation at the vane exit, ω, can be calculated from the following equation:

$$\omega = \frac{V_u}{r} = \frac{V_x \ \mathrm{Tan}\ a}{r}. \qquad \text{Eq (28)}$$

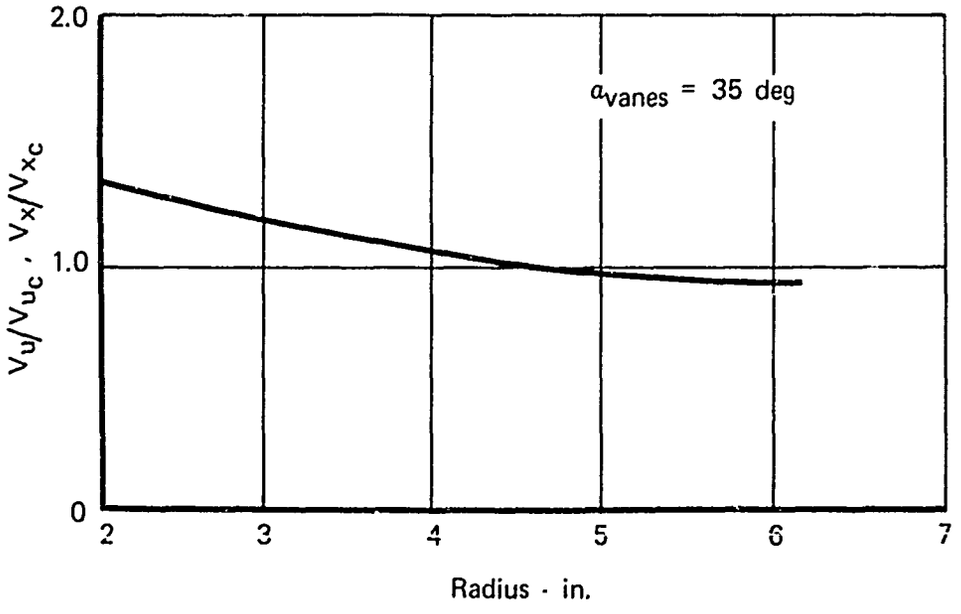

Figure C-1. Radial Variation of Tangential and Axial Velocities in Scaled Swirl Augmentor Tested Under NASA Contract

FD 89710

Downstream of the vanes, the cold, unburned gases are forced toward the center due to the expansion of the burned gases. Since angular momentum is conserved along a streamline, $V_u r$ = constant along a streamline. The rotational rate downstream of the vanes was calculated using this fact, and the analysis is shown below.

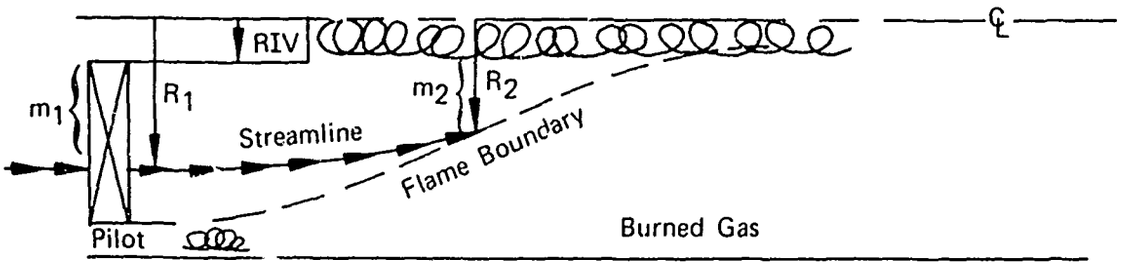

$$\frac{m_1}{m_2} = \frac{\rho_1 A_1 V_1}{\rho_2 A_2 V_2} = \frac{\frac{P_1}{\tilde{R} T_1} (\pi R_1^2 - \pi RIV^2) M_1 \sqrt{\gamma \tilde{R} T_1}}{\frac{P_2}{\tilde{R} T_2} (\pi R_2^2 - \pi RIV^2) M_2 \sqrt{\gamma \tilde{R} T_2}} = 1 \quad \text{Eq (29)}$$

where:

P	Static pressure
$\tilde{R}$	Gas constant
T	Static temperature
M	Mach number
γ	Ratio of specific heats
m	Mass flow

R_1, R_2, and RIV from diagram above.

If $T_1 \equiv T_2$, $\pi R_1^2 - \pi RIV^2 \quad A_1$ and $\pi R_2^2 - \pi RIV^2 = A_2$,

then

$$A_1 \quad A_2 \frac{P_2}{P_1} \frac{M_2}{M_1} . \qquad \text{Eq (30)}$$

From the conservation of angular momentum along a streamline:

$$V_{u_2} = V_{u_1} \frac{R_1}{R_2} .$$

Now

$$\frac{R_1}{R_2} = \frac{\sqrt{A_1 + \pi RIV^2}}{\sqrt{A_2 + \pi RIV^2}}$$

so,

$$V_{u_2} = V_{u_1} \sqrt{\frac{A_1 + \pi RIV^2}{A_2 + \pi RIV^2}} . \qquad \text{Eq (31)}$$

Substituting equation 30 into equation 31 we get

$$V_{u_2} = V_{u_1} \sqrt{\frac{\frac{A_2 P_2 M_2}{P_1 M_1} + \pi RIV^2}{A_2 + \pi RIV^2}} . \qquad \text{Eq (32)}$$

Therefore,

$$\omega_2 = \frac{V_{u_2}}{R_2} = \frac{V_{u_1}}{R_2} \sqrt{\frac{\frac{A_2 P_2 M_2}{P_1 M_1} + \pi RIV^2}{A_2 + \pi RIV^2}} . \qquad \text{Eq (33)}$$

The second term required in equation 4, ρ_B/ρ_a, was assumed constant throughout the burning. If the fuel-air mixture was such that the mixture burned at a stoichiometric flame temperature, the density ratio was 0.393 for an inlet temperature of 1644°R.

The last term required in equation 4, $2V_B/A_B C_D$, was calculated from equation 13 assuming a bubble diameter equal to the pilot dimension. The bubble

Reynolds number was checked to assure the limit size was not reached. The Reynolds number of the bubble, assuming a diameter of 1.15 inches, was

$$Re_{bub} = 174\, S_B \,. \qquad \text{Eq (34)}$$

Therefore, until the bubble reached a velocity of 404 ft/sec, the limiting size would not be reached. The analytical program predicted this velocity would not be reached. Therefore, $2V_B/A_B\, C_D$ was assumed constant and equal to 0.0296.

Once the terms ω, ρ_B/ρ_a, and $2V_B/A_B\, C_D$ were calculated at each axial station, the radial flamespreading rate, including the expansion rate term, was calculated step by step in the following manner. Starting at time zero, the burning rate was calculated using equation 4. For a small increment of time, the amount of flow burned was calculated and the weight flowrate of the hot and cold streams, $\dot{w}_h$ and $\dot{w}_c$, were adjusted accordingly. The hot gases were then allowed to expand into the cold stream. Mathematically, the area occupied by the cold gas, A_c, the area occupied by the hot gas, A_h, and the static pressure were calculated from the following three equations:

$$A_c = \frac{\dot{w}_c \sqrt{T_{t_c}}}{P_{t_c} \sqrt{\frac{2G\gamma}{(\gamma-1)\,\tilde{R}} \left[\left(\frac{P}{P_{t_c}}\right)^{\frac{2}{\gamma}} - \left(\frac{P}{P_{t_c}}\right)^{\frac{\gamma+1}{\gamma}} \right]}} \qquad \text{Eq (35)}$$

$$A_h = \frac{\dot{w}_h \sqrt{T_{t_h}}}{P_{t_h} \sqrt{\frac{2G\gamma}{(\gamma-1)\,\tilde{R}} \left[\left(\frac{P}{P_{t_h}}\right)^{\frac{2}{\gamma}} - \left(\frac{P}{P_{t_h}}\right)^{\frac{\gamma+1}{\gamma}} \right]}} \qquad \text{Eq (36)}$$

$$A_t = A_h + A_c \qquad \text{Eq (37)}$$

where

A	=	area
$\dot{w}$	=	weight flowrate
T_t	=	total temperature
P_t	=	total pressure
P	=	static pressure
γ	=	ratio of specific heats
$\tilde{R}$	=	gas constant
G	=	gravitational acceleration

Subscript c = cold
h = hot
t = total.

In these equations, P_{t_c} was assumed constant, while P_{t_h} deceased axially according to the fraction of mass burned. From the static pressure, the axial velocity was calculated and used to determine the axial movement of the flame bubble. The first step of the burning-expansion process was then complete. Each succeeding step was done in the same manner until all of the gases were burned.

The analytical model of the swirl augmentor was incorporated into a computer program. A listing of the program plus theoretical results of the swirl augmentor tested under NASA Contract NAS3-17348 are presented on the following pages.

```
FORTRAN IV G1  RELEASE 2.0            MAIN                    DATE = 75127          15/13/28                PAGE 0001

0001                  IMPLICIT REAL(M)
0002                  REAL M,MIN,MAX,LENGTH,MOUT,MOUTC                                                    00000010
0003                  R1DOTF   (R1,OMEGA,RHO,COD2L,R1DOT) =-F1*OMEGA**2/PHO*(1.0-RHO) +                   00000020
                     1COD2L/RHO*R1DOT**2                                                                  00000030
0004                  DELTAT = .00005                                                                     00000040
0005                100 READ(5,101,END=99)    R1,TTI,MIN,VANG,GAMMA,D,TADIA,RIV,ROV,PT1,                00000050
                     1TTI                                                                                 00000060
0006                101 FORMAT(7F10.0/4F10.0)                                                           00000070
0007                  WRITE(6,102) R1,TTI,MIN,VANG,GAMMA,D,TADIA,RIV,ROV,PT1,TTI                          00000080
0008                102 FORMAT('1',' R1    = ',F7.2,' IN'/                                              00000090
                     *       ' ',' TTI   = ',F7.1,' DEG-R'/                                               00000100
                     *       ' ',' MIN   = ',F7.5/                                                        00000110
                     *       ' ',' VANG  = ',F7.5,' RAD'/                                                 00000120
                     *       ' ',' GAMMA = ',F7.5/                                                        00000130
                     *       ' ',' D     = ',F7.3,' FT'/                                                  00000140
                     *       ' ',' TADIA = ',F7.1,' DEG-R'/                                               00000150
                     *       ' ',' RIV   = ',F7.3,' IN'/                                                  00000160
                     *       ' ',' ROV   = ',F7.3,' IN'/                                                  00000170
                     *       ' ',' PT1   = ',F7.3,' PSI'/                                                 00000180
                     *       ' ',' TTI   = ',F7.1,' DEG-R')                                               00000190
0009                  SS = SORT(GAMMA*1716.*TTI)                                                          00000200
0010                  R1 = R1 /12.0                                                                       00000210
0011                  ROV = ROV/12.0                                                                      00000220
0012                  RIV = RIV/12.0                                                                      00000230
0013                  CALL ISNFLO(GAMMA,MIN,X,X,X,AL,X,X,X)                                               00000240
0014                  AR=0.94*AL* (ROV**2-RIV**2)/R1**2                                                   00000250
0015                  MO=-1.0                                                                             00000260
0016                  X=0.0                                                                               00000270
0017                  CALL ISNFLO(GAMMA,MO,X,X,X,AP,X,X,X)                                                00000280
0018                  VAXIN=MO*SS                                                                         00000290
0019                  AT = 3.14159*ROV**2- 3.14159*RIV**2                                                 00000300
0020                  I = 0                                                                               00000310
0021                  R1DOT = 0.0                                                                         00000320
0022                  TIME = 0.0                                                                          00000330
0023                  COD2L =35.00                                                                        00000340
0024                  R1 = ROV                                                                            00000350
0025                  RHO = TTI/TADIA                                                                     00000360
0026                  VOUT = VAXIN                                                                        00000370
0027                  LENGTH = 0.0                                                                        00000380
0028                  CONST = VOUT*TAN(VANG)                                                              00000390
0029                  CALL RAYLEY(GAMMA,MIN,TO1,X,PO1,X,X,X)                                              00000400
0030                  TTSTAR = TTI/TO1                                                                    00000410
0031                  TO2 = TADIA/TTSTAR                                                                  00000420
0032                  MOUT = -1.0                                                                         00000430
0033                  PO2=0.0                                                                             00000440
0034                  CALL RAYLEY(GAMMA,MOUT,TO2,X,PO2,X,X,X)                                             00000450
0035                  PTRAT = PO2/PO1                                                                     00000460
0036                  CALL ISNFLO(GAMMA,MIN,X,P,X,X,FUNCT,X,X)                                            00000470
0037                  WT = FUNCT*PT1*AT/SORT(53.3E*TTI/32.17)*144.0                                       00000480
0038                  WC = WT                                                                             00000490
0039                  WF = 0.0                                                                            00000500
0040                  PIN = P*PT1                                                                         00000510
0041                  OMEGA = CONST/R1                                                                    00000520
0042                  R1DOT = R1DOTF(R1,OMEGA,RHO,COD2L,R1DOT)                                            00000530
0043                  WRITE(6,15)                                                                         00000540
0044                15 FORMAT('0',' SPEED  COLD STREAM V      TIME      LENGTH      RADIUS     FLAME00000550
                     *       ' ',' OMEGA      PULK TEMP'/                                                 00000560
                     *       ' ',' (SEC)        (FT)        (FT)      (F00000570
                                                                                                          00000580
```

```
                      *T/SEC)       (FT/SEC)      (RAD/SEC)        (DEG-P)*)                00000*50
0045                  * IF(((I/10)*10-I).EQ.0)                                               00000C00
                       1WRITE(6,12) TIME,LENGTH,R1,RIDOT,VOUT,OMEGA,TT1                      CCOOC*1C
0046                  12 FORMAT(* *,F1*.2,5F15.4)                                            00000E20
0047                     IF(R1.LE.0.0) GO TO 22                                              00000E30
0048                     IF(WC.EQ.0.0) GO TO 22                                              00000E40
0049                     I = I+1                                                             00000E50
0050                     TIME = TIME + DELTAT                                                00000660
0051                     RIDOT = RIDOT*DELTAT + RIDOT                                        00000E7C
0052                     R2 = RIDOT*DELTAT + R1                                              00000EB0
0053                     IF (R2.LE.RIV) R2=RIV                                               00000E9C
0054                     AC = 3.141*9*R1**2 - 3.141*9*RIV**2                                 00000700
0055                     DM = 3.141599*(R1**2-R2**2)/AC*WC                                   00000710
0056                     WC = WC-DM                                                          00000720
0057                     IF(WC.LE.0.0) WC = 0.0                                              00000730
0058                     WM = WT-WC                                                          00000740
0059                     RMIR = WM/WT                                                        00000750
0060                     R2CRIT = RMIR*(PTRAT-1.0)+1.0                                       00000760
0061                     PTM = R2CRIT*PTI                                                    00000770
0062                     P1 = PSTAT(WC,TTI,PTI,AC,MC,WM,TADIA,PTM,AM,RM,AT)                  00000780
0063                     IF(I.EQ.1) P1I=P1                                                   00000790
0064                     TT1 = (WT-WC)/WT*TADIA + WC/WT*TTI                                  00000800
0065                     R1 = SQRT(AC/3.141*9 + RIV**2)                                      00000E10
0066                     VEXP = (R1-R2)/DELTAT                                               00000E20
0067                     IF(MC.EQ.0.0) MC=MM                                                 00000E30
0068                     VOUT = MC*SS                                                        00000E40
0069                     LENGTH = DELTAT*VOUT + LENGTH                                       00000E50
0070                     IF (R1.LE.RIV)                                                      00000E60
                        1WRITE(6,12) TIME,LENGTH,R1,RIDOT,VOUT,OMEGA,TT1                    00000870
0071                     IF(R1.LE.RIV) GO TO 22                                              00000880
0072                     OMEGA =CONST*SQRT((P1/P1I*MC/MIN*AC+3.141*9*RIV**2)/(AC+3.1415*     00000890
                        1*RIV**2))/R1                                                       00000900
0073                     IF (LENGTH.GE.0) GO TO 90                                          00000910
0074                     RIDOT = RIDOTF(P1,OMEGA,PMC,CDC2L,RIDOT)                           00000920
0075                     GO TO 8                                                            00000930
0076                  22 WRITE(6,58)                                                        00000940
0077                  58 FORMAT(*  EFF = 1.0*)                                              00000950
0078                     GO TO 100                                                          00000960
0079                  90 WRITE(6,91)                                                        00000970
0080                  91 FORMAT(* LENGTH EXCEEDS MAXIMUM LENGTH - CASE TERMINATED*)         00000980
0081                     GO TO 100                                                          00000990
0082                  99 STOP                                                               00001000
0083                     END                                                                00001010
```

```
FORTRAN IV G1  RELEASE 2.0            PSTAT            DATE = 71127        14/10/28            PAGE 0001

0001                  FUNCTION PSTAT(WC,TC,PTC,AC,WC,WH,TH,PTH,AH,WH,AT)                    00001020
0002                  IMPLICIT REAL(M)                                                      00001030
0003                  GAMMA = 1.3                                                           00001040
0004                  CALL ISNFLO(GAMMA,1.0,Y,PR,X,X,FC,X,X)                                00001050
0005                  PSTATX = 0.9999*PTH                                                   00001060
0006                  PSTATC = PR*PTC                                                       00001070
0007                  PSTAT1 = PSTATC+0.5*(PSTATX-PSTATC)                                   00001080
0008                  AC = 0.0                                                              00001090
0009                  IF(WC.GT.0.0) AC = WC*SQRT(53.3*TC/32.17)/(PTC*FC)/144.0              00001100
0010                  PR=PSTATC/PTC                                                         00001110
0011                  X=0.0                                                                 00001120
0012                  WH=-1.0                                                               00001130
0013                  FH=0.0                                                                00001140
0014                  CALL ISNFLO(GAMMA,WH,X,PR,X,X,FH,X,X)                                 00001150
0015                  AH = 0.0                                                              00001160
0016                  IF(WH.GT.0.0) AH = WH*SQRT(53.35*TH/32.17)/(PTH*FH)/144.0             00001170
0017                  Z = AT-AC-AH                                                          00001180
0018                  KOUNT=1                                                               00001190
0019                  PSTAT = PSTAT1                                                        00001200
0020                  IOPT=0                                                                00001210
0021                1 WH=-1.0                                                               00001220
0022                  X=0.0                                                                 00001230
0023                  IF(PSTAT.GT.PTH) PSTAT=PTH                                            00001240
0024                  PR=PSTAT/PTH                                                          00001250
0025                  FH=0.0                                                                00001260
0026                  CALL ISNFLO(GAMMA,WH,X,PR,X,X,FH,X,X)                                 00001270
0027                  AH = 0.0                                                              00001280
0028                  IF(WH.GT.0.0.AND.FH.GT.0.0)                                           00001290
                     1 AH=WH*SQRT(53.35*TH/32.17)/(PTH*FH)/144.0                          00001300
0029                  WC=-1.0                                                               00001310
0030                  X=0.0                                                                 00001320
0031                  PR=PSTAT/PTC                                                          00001330
0032                  FC=0.0                                                                00001340
0033                  CALL ISNFLO(GAMMA,WC,X,PR,X,X,FC,X,X)                                 00001350
0034                  AC = 0.0                                                              00001360
0035                  IF(WC.GT.0.0) AC=WC*SQRT(53.35*TC/32.17)/(PTC*FC)/144.0               00001370
0036                  IF(IOPT.EQ.2) RETURN                                                  00001380
0037                  Z=AT-AC-AH                                                            00001390
0038                  CALL SOLVIT(PSTATC,ZC,PSTAT,Z,KOUNT,IOPT,SAVE01,SAVE02)               00001400
0039                  KOUNT = KOUNT + 1                                                     00001410
0040                  IF(KOUNT.GT.2000) GO TO 3                                             00001420
0041                  IF(PSTAT.LE.PTH.AND.PSTAT.GE.PSTATC) GO TO 1                          00001430
0042                4 WRITE(6,2) WC,TC,PTC,AC,WC,WH,TH,PTH,AH,WH,AT,PSTAT,Z               00001440
0043                2 FORMAT(' *** ERROR IN FUNCTION PSTAT - ARGUMENTS ARE - '/            00001450
                     * ' ',11E12.6/' ***     PSTAT = ',F12.7,'      AREA ERROR = ',E14.7)  00001460
0044                  RETURN                                                                00001470
0045                3 WRITE(6,4)                                                            00001480
0046                4 FORMAT(' *** NO SOLUTION IN PSTAT')                                   00001490
0047                  GO TO 5                                                               00001500
                C     DEBUG UNIT(6),TRACE,INIT                                            00001510
                C     AT 1                                                                00001520
                C     TRACE ON                                                            00001530
0048                  END                                                                   00001540
```

R1 = 7.900 IN
TT1 = 1644.0 DEG-R
MIN = 0.11500
VANG = 0.61000 RAD
GAMMA = 1.30000
D = 15.000 FT
TADIA = 4172.0 DEG-R
RIV = 2.000 IN
ROV = 6.333 IN
PT1 = 30.000 PSI
TT1 = 1644.0 DEG-R

TIME (SEC)	LENGTH (FT)	RADIUS (FT)	FLAME SPEED (FT/SEC)	COLD STREAM V (FT/SEC)	OMEGA (RAD/SEC)	BULK TEMP (DEG-R)
0.0	0.0	0.5278	0.0	370.0693	490.0964	1644.0000
0.000500	0.1126	0.4985	-47.6880	231.6797	530.4905	1832.6670
0.001000	0.2329	0.4547	-52.4669	252.3921	601.6831	2098.0913
0.001500	0.3672	0.4102	-57.5394	278.9834	695.7451	2356.2004
0.002000	0.5151	0.3637	-63.4271	309.9822	814.7407	2699.6582
0.002500	0.6793	0.3173	-70.2008	343.8943	962.1321	3037.0801
0.003000	0.8609	0.2710	-77.2003	379.1724	1141.7449	3391.1707
0.003500	1.0601	0.2240	-83.4612	414.0359	1349.9583	3747.2451
0.004000	1.2761	0.1801	-85.9835	442.5482	1533.1875	4079.3823
0.004200	1.3666	0.1667	-83.7784	454.7400	1551.8916	4172.0000

EFF = 1.0

REFERENCES

1. Davies, R. M., and Sir Geoffrey Taylor, Proceedings of the Royal Society, London, A200, 375, 1950.

2. Levy, A., Proceedings of the Royal Society, London, A238, 134, 1965.

3. Haberman, W. L. and R. K. Morton, An Experimental Investigation of the Drag and Shape of Air Bubbles Rising in Various Liquids, Navy Department. Report 802, September 1953.

4. Uno, Seiji and R. C. Kinter, Effect of Wall Proximity on the Rate of Rise of Single Air Bubbles in a Quiescent Liquid, A.I.Ch.E. Journal, September 1956.

5. Wegner, Peter P., et al., Spherical Cap Bubbles Rising in Liquids, Journal of Aeronautics, 1971.

6. Turbine Design and Application, Edited by Arthur J. Glassman, NASA Lewis Research Center, Volume 1, 1972.